Analysis of Interference in LFM Radar Detection and Imaging in a Multi-Radar Environment

By

Suanu Nwigbo

Department of Electrical and Computer Engineering

School of Engineering and Digital Science (SEDS)

Nazarbayev University,

Astana

A thesis submitted to the School of Engineering and Digital Sciences (SEDS) of Nazarbayev University in Partial Fulfillment of the Requirements for the Degree of

Master of Science in Electrical and Computer Engineering

Nazarbayev University

April, 2023

Originality Statement

I, Suanu Nwigbo, hereby declare that this submission is my own work and to the best of my knowledge it contains no materials previously published or written by another person, or substantial proportions of material that have been accepted for the award of any other degree or diploma at Nazarbayev University or any other educational institution, except where due acknowledgment is made in the thesis.

Any contribution made to the research by others, with whom I have worked at NU or elsewhere is explicitly acknowledged in the thesis.

I also declare that the intellectual content of this thesis is the product of my own work, except to the extent that assistance from others in the project's design and conception or in style, presentation, and linguistic expression is acknowledged.

Signed on 15.04.2023

_____

Abstract

Because of the growing use of radio detection and ranging (radar) systems in multiple application sectors, the radars have to be operated on the same or adjacent frequency resources. This frequency overlap can cause interference and impacts the performance of the victim radar. Besides unintended interferences, there could also be intentional interferences. The interference can cause a reduction in the signal-to-noise ratio, introduce ghost targets, and lead to poor detection capabilities of the radar as well as false detections. Thus, interference effects should be compensated to operate the radar in a safe and secure environment.

In this thesis, different types of interference and their impact on traditional linear frequency modulation (LFM) based radio detection and ranging (radar) are investigated through numerical simulation and electronic radar-based experiments. The work has been extended to investigate the imaging of radar-detected objects with the help of the back-projection technique.

In the simulation environment, a multi-radar environment has been created to investigate the effect of external interference radar on the victim radar. Different types of interference waveforms such as LFM, triangular and pulsed waveforms are being considered. It is found that the LFM-based waveform suffers from coherent LFM interference, which can result in the appearance of ghost targets on the range profile. Whereas, non-coherent types of interference increase the noise level, reducing the signal-to-noise ratio, thus adversely impacting the detection accuracy. Thus, a random hopping LFM-based waveform as an alternative to the LFM-based waveform has been proposed as a robust waveform to mitigate interference in a multi-radar environment.

Experimental work with an mm-wave (77GHz-81GHz) radar sensor for detecting targets has been performed, and radar performance metrics such as range and range resolution have been evaluated with the theoretical values.

Through the back-projection algorithm, the imaging of the detected objects has been obtained. Through extensive iteration, it is found that the back-projection with weighting function provides enhanced resolution.

Acknowledgments

This thesis is dedicated to my lovely wife Hassanat, and my daughters Sira and Zina to whom I owe so much for their endurance and faith in me. I know that they will follow the right path in life and become good people. To Mum and Dad for their love, care, and support, sister Ere and her husband Phil. To Legian and Sincto, to inspire them that there is surely a silver lining in every grey cloud, to my supervisor Prof. Ikechi Ukaegbu and an external co-supervisor from Nanjing University of Aeronautics and Astronautics, Nanjing, China, Prof. Bikash Nakarmi. Finally, to my friends in the IDSN lab: Ravi, Elo, Nazym, Dimash, and all those whom I couldn't mention. I am thankful for your support and friendship during the course of the program.

List of Abbreviations

ADC – Analog to Digital Converter

ABS- Automatic Brake System

ACC-Automatic cruise control

ADAS-Advanced Driver Assistance System

ADS-Automatic driverless system

AV- Autonomous Vehicle

CP- Cyclic Prefix

CW-continuous wave

DSP- Digital Signal Processing

FFT-Fast Fourier transform

GPR-Ground penetrating radar

HPB-Half power Bandwidth

FOV-Field of view

IBP-Incoherent back Projection

NHTSA-National highway safety administration

OFDM-Orthogonal frequency division multiplexing

IFFT- Inverse fast Fourier transform

PMCW-pulse modulated continuous wave

PRF-Pulse repetition frequency

PRI-Pulse repetition interval

PSD-power spectral density

SAR-Synthetic Aperture Radar

SAE-Society of automotive engineers

SNR-Signal-to-noise ratio

SDK-Software development kit

TABLE OF CONTENTS

List of Tables

List of Figures

Chapter 1- Introduction

1.1 General

Radio detection and ranging is a sensing method that relies on the reflective power of electromagnetic waves on solid objects to track, estimate and determine the objects' range, radial velocity, and angular orientation in real-time. Initially developed for military purposes, radar has come a long way, finding its way into civilian applications like weather forecasts, speed tracking, satellite imaging, and autonomous vehicles. The last application area operates in the millimeter wave range[1],[2],[3] at frequencies of several Gigahertz, and is the interest of this research. The basic configuration of a radar system is as shown below:

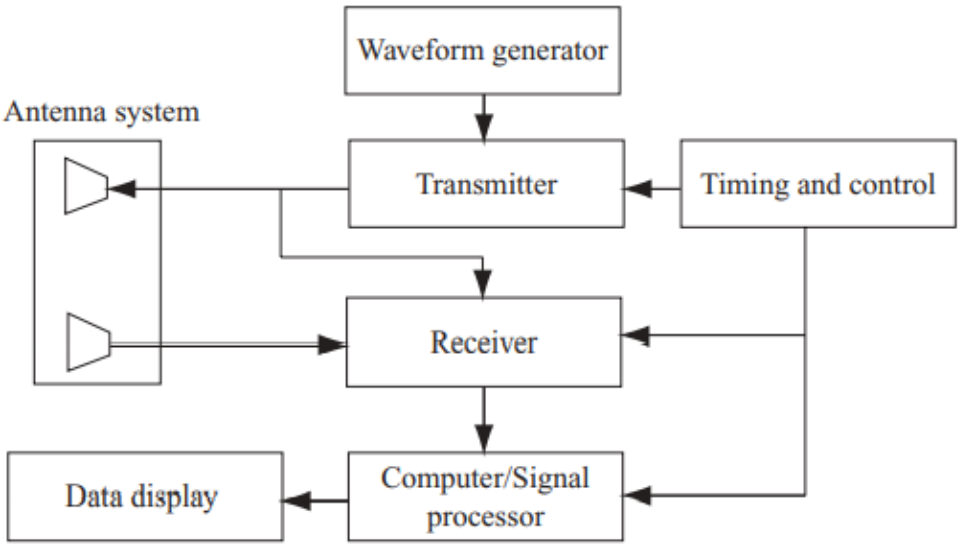

Fig 1.1. Radar system block diagram [4].

The waveform generator produces the electromagnetic waves that are sent outwards by the transmitter towards the targets while the antenna directs the e/m waves for transmission, The receiver collects the reflected waves from the target objects' echoes and sends it to the signal processing unit of the system. Timing and control are necessary to differentiate the transmitted

cycle from the receiving cycle as well as to perform other resetting procedures necessary for the effective working of the radar. The basic workings of the radar is as shown below:

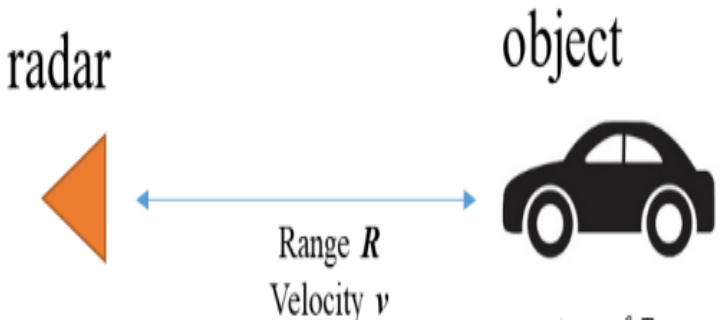

Fig 1.2. Basic radar system [5].

For a given isotropic antenna, the power density received at the receiver antenna from a target with a given cross-sectional area (receiver cross-sectional RCS) is given by the following equation:

$$S = \frac{p_t G^2 \lambda^2 \alpha}{(4\pi)^3 R^2} \mathrm{L} \qquad (1)$$

Where p_t is the transmitted power at the antenna, G is the antenna gain, λ is the wavelength of the transmitted signal, α is the target object's cross-sectional area, R is the radial distance of the target object from the antenna and receiver and L is a positive number less than one that accounts for the losses due to power dissipation and equipment imperfections.

Equation 1 is called the radar range equation as it expresses the received power as a function of radial distance R. The radar cross-section α is a function of the target object's size as well as the transmitter's field polarity. The relationship between α and the polarity of the transmitted electric field is as follows:

$$\begin{bmatrix} E_H^r \\ E_V^r \end{bmatrix} = \begin{bmatrix} \alpha_{HH} & \alpha_{VH} \\ \alpha_{HV} & \alpha_{VV} \end{bmatrix} \begin{bmatrix} E_H^r \\ E_V^r \end{bmatrix} \qquad (2)$$

With the subscripts V and H denoting the vertical and horizontal polarization components of the electric field respectively. In most radar applications, the receiver and transmitted signals are polarized in one dimension together, thus only one of the four matrices entries are present, giving a single scaler value for RCS. Typical values of object RCS are shown in the table below:

Table 1. Typical RCS values of common objects.

Unit	Insects	Birds	Humans	Aircraft	Ships
m^2	0.001	0.01	0.1	100	10,000
dBsm	-30	-20	-10	20	40

In order to deploy a radar sensor for any application, the radar maximum unambiguous range must be correctly computed. This parameter determines the farthest distance that target objects can be located in order to be correctly detected by the transmitter/receiver antenna.

From equation (1), the maximum unambiguous distance of the radar can be computed as:

$$D_{max} = \frac{P_t G_t G_r \lambda^2}{(4\pi)^3 R^3 * PRF} \quad . . \quad . \quad .(3)$$

PRF is the pulse repetition frequency, R is the target object distance from the radar, G_r, G_t are the antenna receiver and transmitter gain respectively. For an object located R meters from the receiver antenna, R can be computed by the following equations:

$$R = \frac{c\tau}{2} \ldots \quad (4)$$

Where, c is the velocity of electromagnetic waves in air ($3*10^8$ m/s)

T is the round trip time for the wave to go from the antenna to the target and back.

The object velocity can then be computed by analyzing various return echoes from the target object and evaluating the frequency change (f_D) in the received signal:

$$f_D = \frac{V_{rs}}{\lambda_s} \quad , \quad . \quad . \quad (5)$$

Where, V_{rs} is the velocity of the target object with respect to the receiver while λ_s is the signal wavelength.

The pulse repetition frequency as well as the transmitted and received pulse of a simple radar system are shown in Fig. 1.3.

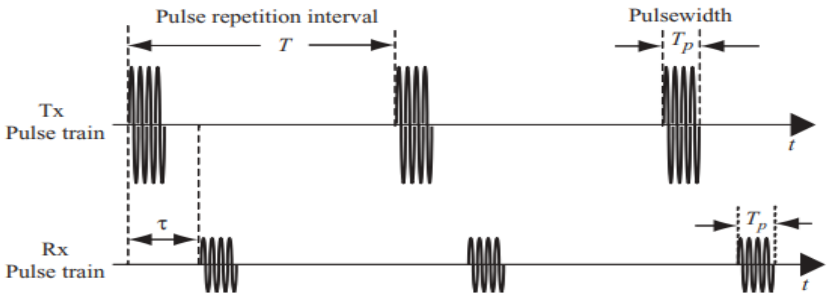

Figure 1.3. Basic signal transmission in a radar system [4].

Radar technology has undergone remarkable advancements in recent years, revolutionizing various fields such as defense, aviation, meteorology, and autonomous systems. Radars are instrumental in providing valuable information about the surrounding environment, enabling accurate detection, tracking, and imaging of targets[6]. Among the different radar waveforms, Linear Frequency Modulated (LFM) radar has gained significant popularity due to its favorable characteristics, including high range resolution and good target discrimination. Linear frequency modulated signals (LFM) are ubiquitous in many civilian radar applications, especially in the emerging autonomous vehicle [7] markets where they are used by sensors that enable target detection, range, velocity, and orientation. Its popularity stems from the satisfaction of the contrasting range resolution (high bandwidth) and high range (long pulse-width) requirements, making it the most popular pulse compression technique.

LFM radar systems emit a waveform with a linearly increasing or decreasing frequency over time, allowing for precise range measurements and the ability to distinguish multiple targets in close proximity. These radars operate by transmitting a modulated waveform and detecting the echo reflected from the targets. The received signal is then processed to extract relevant information, such as range, velocity, and angular position of the targets.

However, with the increasing deployment of radar systems worldwide, the issue of interference between radars operating in close proximity has emerged as a significant concern. Interference occurs when the transmitted signals from one radar system interfere with the signals received by another radar system, leading to performance degradation and compromised functionality. In a multi-radar environment, where multiple radars operate simultaneously, the likelihood of interference incidents increases substantially.

The interference in radar systems can stem from various sources, including co-located radar systems, adjacent radar installations, or unintentional transmissions from other electronic devices operating in the same frequency band. When multiple radars emit overlapping signals, the echoes from different targets can become intertwined, resulting in interference that manifests as false targets, degraded signal-to-noise ratio, reduced range resolution, and compromised imaging capabilities.

The consequences of interference in radar systems can be severe, particularly in critical applications such as air traffic control, military surveillance, and weather monitoring. Interference can lead to inaccurate target detection, false alarms, missed detections, and reduced situational awareness, which can have serious implications for decision-making and operational safety. Therefore, it is imperative to understand the nature of interference in LFM radars operating in a multi-radar environment and develop effective mitigation strategies to ensure reliable and robust radar operation.

The successful deployment of vehicle sensors utilizing this pulse compression technique led to the development of millimeter wave radars (short wavelength electromagnetic waves) by companies like Tesla and Texas Instruments. Most automotive radars operate in the millimeter wave band as shown in the frequency spectrum below:

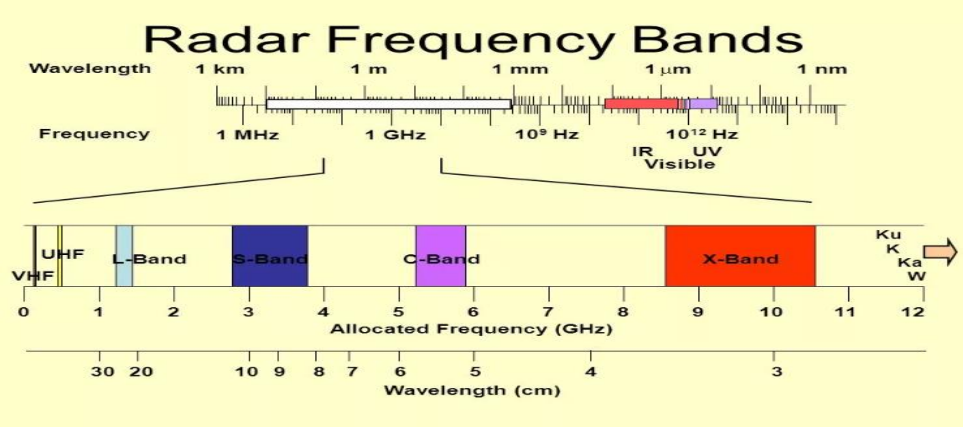

Fig 1.4. Millimeter wave bands used for autonomous vehicles [4].

1.2 Problem definition

Radar sensors and transmitters must operate in a given frequency range of the electromagnetic spectrum. This means that frequency overlap must occur in the course of utilizing these sensors. As more car manufacturers fit their devices with radar sensors, it is inevitable that transmitted signals will overlap from one vehicle to another, causing confusion between received signals and externally transmitted signals. This situation is known as interference in a multi-radar environment. The possibilities of false detection, unexplained noise levels and object misclassification all become real.

In order not to defeat the purpose for which the radar sensors were fitted to the vehicles in the first place, it is important that the interference signals responsible for the radar underperformance/error are fully investigated and analyzed. This work aims to undertake this objective through software simulation and experimental validation.

1.3 Objectives of the Thesis

The objective of this thesis is to analyze the type, nature and effects of interferences on LFM signals in a multi-radar environment as well as their impact on radar imaging. The interferences studied are not confined to LFM wave sources alone but are extended to pulse, triangular and frequency-hopped LFMs.

Research methodology: The research methodology adopted in this thesis are as follows:

- Conduct a comprehensive review of the state-of-the-art in terms of current practice in the field. This review will involve understanding the interferences that occur in LFM systems operating in multi-radar environments as well as the methods used in developing images from radar signals.

- Develop a model of the interference scenarios using mathematical equations. The system model will include the equations for the transmitted, received and interference signal as well as the radar transmitter power and range equations.

- Analyze the interference situations that occur in a multi-radar environment on an LFM signal. The analysis includes the identification of the interference signal characteristics, parameters and waveforms as well as the influence of these parameters on the radar system performance. The impact of this interference on object detection, SNR and image resolution will also be analyzed.

- Perform an experiment using the Texas Instrument millimeter wave radar sensor IWR1843 to compare the range detection alongside the simulation result, with further research into the interference dynamics as well as Doppler evaluation and image processing to follow.

1.4 Thesis structure

Chapter 2 serves as a preamble to introduce and explain key terminologies and parameters used in radar systems. The aim is to make further dissection of the literature easier for the readers.

Chapter 3 gives an extensive literature review on LFM radars used in automotive applications. Some analysis of interference in multi-radar situations are also examined with emphasis on key performance metrics over the course of time. Various aspects of radar systems are analyzed, including the various waveforms being used nowadays and the nature of interferences.

Chapter 4 discusses the literature on radar imaging and a few popular algorithms in use as well as some background of the dataset used in the research experiment. The Texas Instrument millimeter wave radar IWR1843 alongside the DCA 1000EVM board are examined because they were used in the experiments to validate the radar's performance in order to compare with the simulation results.

Chapter 5 discusses the work done on the experimental data from back projection imaging experiment as well as the attempt to improve the final image using the hamming window algorithm .Finally, chapter six is the conclusion as well as future work to be done.

Chapter 2- Fundamentals of Radar

In order to carry out a synthesis of LFM radar systems and their interference dynamics, it is important to understand some terminologies and parameters. This is done to make subsequent understanding of the thesis easier.

2.1 LFM parameters

LFM signals are the most popular waveform employed in automotive radar applications. A non-exhaustive generic list of some important terms and parameters associated with this waveform are as below:

2.1.1 Chirp

A chirp for an LFM signal is a description of the characteristics of the signal during one transmission period. It consists of a signal with a starting frequency whose value changes linearly throughout the period of the cycle. Mathematically, a chirp can be written as follows:

$$s(t) = A * \cos[2\pi(f_0 t + \frac{1}{2}\alpha t^2)] \text{ .....(6)}$$

Where:

$s(t)$ represent the chirp signal at time t.

A is the amplitude of the chirp signal.

f_0 is the starting frequency of the chirp.

α represents the rate of change of frequency with time (chirp rate)

The Bandwidth (B) divided by the chirp sweep-time is the chirp

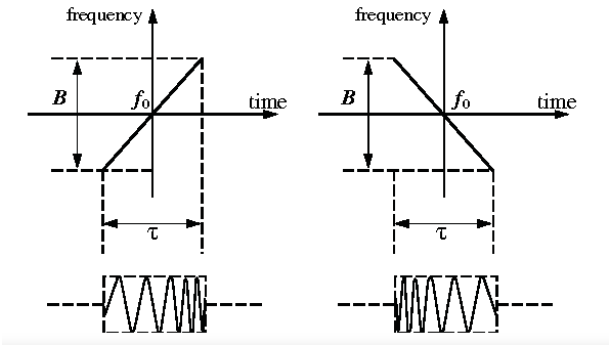

Fig 2. LFM signal showing an upward ramp (L) and a downward ramp (R).

By changing the value of alpha, various types of waveform can be obtained, depending on the application, for example, a zero value alpha represents a constant frequency wave while a positive alpha value represents a ramp. Lastly, a negative value of alpha represents a downward ramp. Chirp signals find applications in a wide range of fields, including radar systems, sonar systems, communication systems, and medical imaging. They are particularly useful in situations where frequency diversity is required, such as range measurement, target detection, velocity estimation, and imaging[8]. Other parameters associated with the chirp are defined as below:

- Sweep Rate: The rate at which the frequency changes over time, expressed in Hz/s or kHz/ms.
- Instantaneous Frequency: The frequency of the LFM signal at any given moment in time.
- Pulse Repetition Interval (PRI): The time interval between consecutive LFM pulses.
- Pulse Width: The duration of an individual LFM pulse.
- Duty Cycle: The ratio of pulse width to the pulse repetition interval, typically expressed as a percentage.
- Peak Power: The maximum power level attained by the LFM signal.
- Pulse Compression Ratio: The ratio of the uncompressed pulse width to the compressed pulse width, used to enhance target range resolution.
- Range Resolution: The ability of the LFM signal to distinguish between two closely spaced targets along the radar range.
- Target Range: The distance from the radar system to the target.
- Pulse Compression: A technique used to compress the transmitted LFM pulse to improve range resolution.
- Doppler Shift: The change in frequency of the LFM signal due to the relative motion between the radar system and the target.
- Doppler Frequency: The frequency shift caused by the Doppler Effect, proportional to the target's radial velocity.
- Maximum Unambiguous Range: The maximum distance at which a target can be detected without ambiguity in range measurement.
- Minimum Detectable Range: The smallest distance at which a target can be reliably detected.

- Signal-to-Noise Ratio (SNR): The ratio of the signal power to the noise power in the received LFM signal.
- Ambiguity Function: A mathematical function that characterizes the radar system's ability to resolve targets in range and Doppler simultaneously.
- Signal Processing Gain: The improvement in signal detection and range resolution achieved through signal processing techniques, such as matched filtering[9].

These parameters collectively define the characteristics and performance of an LFM signal and are essential for designing and analyzing LFM-based systems.

2.1.2 INR

The interference-to-noise ratio (INR) is a measure of the performance of electronic signals plagued by noise and/or interference. Since the process of transmitting electronic or photonic signals through a medium is not seamless, some external unwanted energy sources always manage to plague the signal of interest. These interfering signals can distort or mask the desired radar signal, making it more challenging to extract meaningful information from the received signal.

On the other hand, noise refers to random fluctuations or disturbances present in the radar system that can affect the clarity and accuracy of the received signal. Background noise in a radar system can come from several sources, including thermal noise, receiver noise, and atmospheric noise. Radar signals must overcome the combination of these energy sources, usually by some filtration methods to stifle the interference while amplifying the signal of interest.

The INR is a measure of the relative strength of interference compared to the background noise[10]. A higher INR indicates that the interfering signals are relatively stronger compared to the background noise, making it more difficult to detect and extract the desired radar signal. Conversely, a lower INR implies that the desired signal is more distinguishable from the interfering signals and noise, leading to better radar performance.

To calculate the INR, the power of the interfering signals is divided by the power of the background noise. The power of the interfering signals can be estimated based on their strength or by analyzing their spectral characteristics. The power of the background noise is typically determined by measuring the noise level during periods when no significant signals are present.

The INR is an essential parameter in radar system design and performance evaluation. It helps determine the system's sensitivity, detection range, and overall reliability. A radar system with a high INR may suffer from decreased detection range and increased false alarm rates, as the interfering signals can mask or mimic the desired targets. Therefore, minimizing interference and optimizing the signal-to-noise ratio are crucial for improving the performance and accuracy of LFM radars.

2.1.3 SNR

It is inevitable that the signal of interest and the background noise/interference will merge in the process of processing the LFM signal. The Signal-to-Noise Ratio (SNR) represents the ratio of the desired radar signal's power to the power of background noise. It is a fundamental parameter used to evaluate the quality and reliability of radar systems[11]. A higher SNR implies a stronger and more distinguishable signal, making it easier to detect and extract useful information from the received radar signal. Conversely, a lower SNR indicates that the desired signal is weaker and more susceptible to being obscured or distorted by noise, making it more challenging to discern.

Mathematically, the SNR can be expressed using the following equation:

$$SNR = P_{signal}/P_{noise} \quad \text{.....(7)}$$

Where: SNR is the signal to noise ratio, P_{signal} is the power in the radar signal and P_{noise} is the background noise.

It is often useful to use logarithmic scales in defining SNR:

$$SNR_{decibel} = 10 * \log(SNR) \text{.....(8)}$$

A higher $SNR_{decibel}$ value indicates a better signal quality and a lower level of noise interference. Conversely, a lower $SNR_{decibel}$value indicates a poorer signal quality and a higher level of noise interference**.**

2.1.4 PSD

One of the many advantages of frequency analysis over time domain is the behavior of the signal over a given frequency spectrum. In LFM (Linear Frequency Modulated) radars, the power spectral density (PSD) is a measure of the power distribution across different frequencies in the radar signal. It provides information about the energy content of the radar signal at different

frequency components[12]. Understanding the PSD is crucial for analyzing the radar system's performance, interference mitigation, and signal processing characteristics.

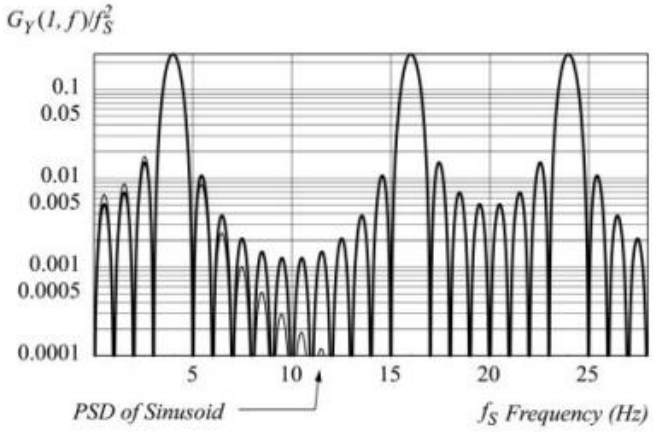

Fig 2.1. PSD of a sampled sinusoid signal [13].

Mathematically, the power spectral density can be written as follows:

$$PSD(f) = |S(f)|^2 \quad \text{.....(9)}$$

A single chirp with the conventional trigonometrical representation can be transformed into its frequency domain representation thus:

$$S(f) = \frac{A}{2}\left(e^{j2\pi\left(f_c-\frac{B}{2T}\right)T} * Sinc\left(\pi t\left(f - f_c + \frac{B}{2\pi}\right)\right) - e^{j2\pi\left(f_c+\frac{B}{2T}\right)T} * Sinc\left(\pi t\left(f - f_c - \frac{B}{2\pi}\right)\right)\right)$$

..... (10)

Where $Sinc(x) = \frac{Sin(\pi x)}{\pi x}$

2.1.5 RHLFM

Random hopped LFM (RHLFM) signals are defined by their varying frequency over time, which is achieved by using a frequency-modulated waveform that randomly switches between several frequency levels. Frequency hopping's randomization offers robustness against interference and lowers the likelihood that enemies may discover the signal Radar systems, communication systems, and wireless sensor networks are just a few of the applications where random hopped linear frequency modulation (LFM) signals have attracted a lot of interest. These signals have benefits like better signal-to-noise ratios (SNRs), robustness against interference, and increased

spectrum usage. RHLFM as a variant of the conventional LFM signal is used in this thesis work to analyze the interference effects in the face of another conventional LFM signal.

2.1.6 FOV

The field of view (FOV) for a radar defines the angular extent of the physical space that the radar system can observe. It encompasses the azimuthal and elevation angles within which the radar can detect, track, and measure targets[14]**.**

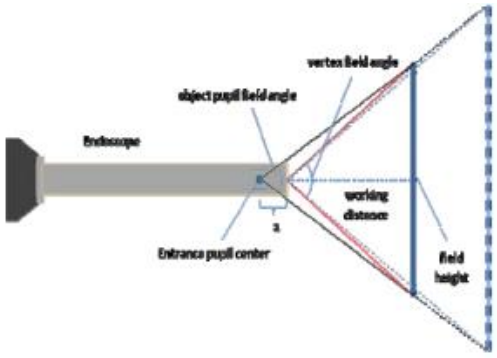

Fig 2.2. Antenna field of view showing object filed angle that make up the cone[15].

The FOV is influenced by factors such as antenna beam-width, scanning capabilities, range considerations, and application-specific requirements. It is a critical parameter that determines the radar's coverage area, target detection capabilities, and overall surveillance effectiveness.

2.1.7 Matched filters

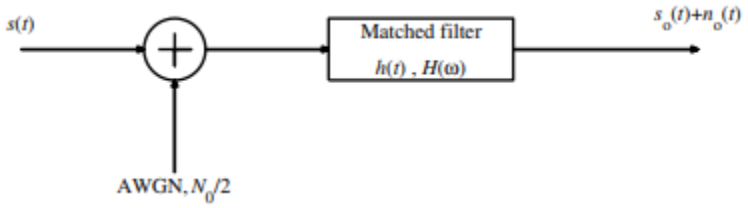

Fig. 2.3. A matched filter response is determined by the delay and input signal[16].

In order to diminish the effect of noise and interference in the receiver section of the radar, a filter with a response matching the transmitted LFM waveform is used. The matched filter response to the target signal is at a maximum when the received signal exactly matches the LFM waveform .implying that the SNR will be enhanced, thus enabling enhanced detection. In radar receiver

design, a threshold level is usually chosen and applied to the output of the filter. Any signal exceeding this threshold is considered to be a target while those below is considered to be noise.

2.1.8 Low pass filter

The extraction of information from the received echo from a target is done by the convolutional operation of the transmitted and received signal, accomplished by the previously discussed matched filter.

To extract this information, the received signal is first mixed with a reference signal that matches the transmitted waveform. This mixing process, known as down-conversion or demodulation, converts the frequency-modulated signal into a baseband signal centered around zero frequency.

However, the demodulated signal contains not only the desired baseband signal but also unwanted high-frequency components resulting from the mixing process. These high-frequency components can arise from the Doppler Effect caused by moving targets or other sources of interference.

To remove these unwanted high-frequency components, a low-pass filter is employed. The low pass filter[17] allows only the low-frequency components of the baseband signal to pass through, attenuating or eliminating the high-frequency components**.**

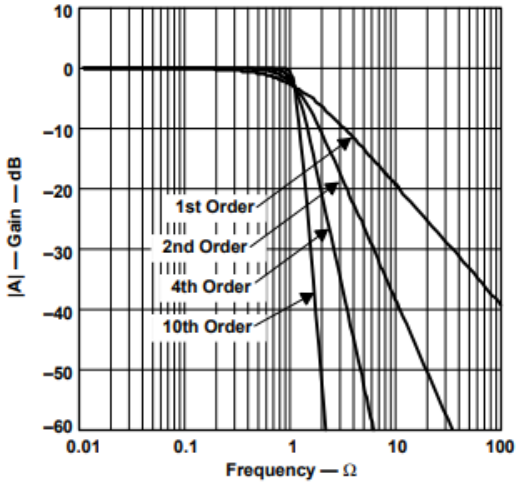

Fig 2.4. Low pass filter characteristic [18].

The low pass filter typically has a cutoff frequency that determines the point at which the attenuation of the high-frequency components begins. Frequencies below the cutoff frequency are passed through with minimal attenuation, while frequencies above the cutoff are progressively

attenuated. By applying a low pass filter to the demodulated signal, the radar system effectively filters out unwanted high-frequency noise and interference, allowing the subsequent signal processing stages to focus on extracting the desired target information accurately**.**

2.2. Summary of chapter

This chapter served to explain the fundamental terms and parameters necessary to understand the discourse on radar. They are by no means exhaustive but have been included as they either feature in the body of the thesis or are drawn from the bigger radar literature. From a signal processing perspective, these devices and concepts form the central theme in the discussion of the dynamics of LFM radar and interference. By briefly giving their description and application, the rest of the thesis can be better understood.

Chapter 3 – Analysis and Simulation of Effect of Interferences on LFM-based Radar

This chapter will examine some of the research done in the field of LFM radars used for automotive applications. The existing research into the literature will throw more light into the important parameters and methods being employed by researchers and will serve as a pivot point for the research objectives outlined in the onset of this thesis by the author. Arising from the research, the simulations and experiments will be drawn and the results explained as a contribution to the research field.

3.1 System autonomy

In figuring out the place of radar sensors in autonomous vehicle schemes, it is important to understand the strengths and weaknesses of the sensors with respect to a human driver. In order to do this, questions like the role of each sensor, their hierarchies, and integration into the overall scheme must first be outlined. One of the most exhaustive research made in this direction was done by Brandon Shoettle. Some of the key areas of research included the analysis of different sensors and their strengths/limitations when fitted to an autonomous vehicle (AV), the comparison of the AV with a human driver under ideal conditions as well as a treatment of the performance of various sensors under the line of sight problem[16].

The review starts from a table provided by the National Highway Safety Administration (NHTSA) in the USA in 2016 in which the level of vehicle automation, levels of engagement required by the driver etc were ranked (See Table 2).

Although a figure of merit is hard to place on the performance of a human operator (driver), a comparison could be made with the assumption that the driver performed optimally, thus scenarios of weaknesses like darkness or low illumination, and physical dirt were not assumed for the driver. Once these conditions were put in place, a reasonable evaluation of the performance of autonomous vehicle sensors with respect to a human driver can be made.

One such area is the limitation of the sensors' FOV, leading to what is called 'blind spots'. This can lead to a situation where two vehicles fitted with sensors (LIDAR, radar, camera) will not

detect the presence of the other even when they are in the sensor range of each other as shown in Fig. 3.0.

Table 2. Degree of classification of vehicle automation [16].

Automation level:	0	1	2	3	4	5
Description:	No automation	Driver assistance	Partial automation	Conditional automation	High automation	Full automation
Driver engagement:	Responsible for all driving	Hands -or- feet off	Hands + feet off (partial)	Eyes off	Brain off (or driver not even present)	
Driver support:	*none*	*Advanced driver-assistance systems (ADAS)*			*only when or if human driven*	
Monitors driving:	*Human driver*			*Automated system*		
Vehicle control:	*Human driver*		*Shared*		*Automated system*	

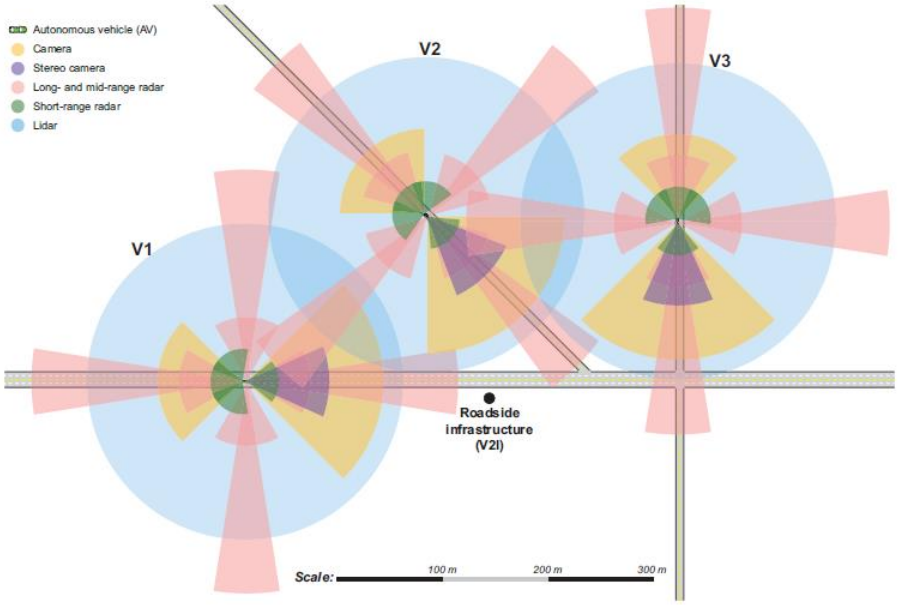

Fig 3.0. Scenario where AV are in sensor distance but still blind to each other's' presence [16].

The conclusions of this white paper were the observations that certain tasks were more suited to machines/sensors, especially concepts like reaction time, consistency and information processing while humans were more adapted in situations requiring intuition and reasoning. It thus served as

a guide towards the need to integrate or assist machines with human intervention, or vice-versa with the ultimate goal of transiting to a fully independent AV in the future.

The Society of Autonomous Engineers (SAE) is one of the research bodies that focus on the levels of autonomous driving as well as the sensors required to achieve these performance levels. Such vehicles are said to be automated driving systems (ADS) and five levels of automation were defined by the SAE. Jaleasa Grayned in his paper [17] reviewed this possibility with the added requirements of the driver at each level. He listed the radar, LIDAR, camera, and ultrasonic sensors as the sensor types suited for the tasks.

3.2 Beam forming and antenna requirements

Having established a clear strategy for the radar sensor in autonomous vehicles, researchers moved to the design of antennas and sought to maximize the signal coverage area through the beam forming techniques.

Beamforming is a technique used in radar antenna design to focus the transmitted radar energy in a specific direction or region of interest. It involves the coherent combination of multiple individual antenna elements to form a beam that can be steered electronically.

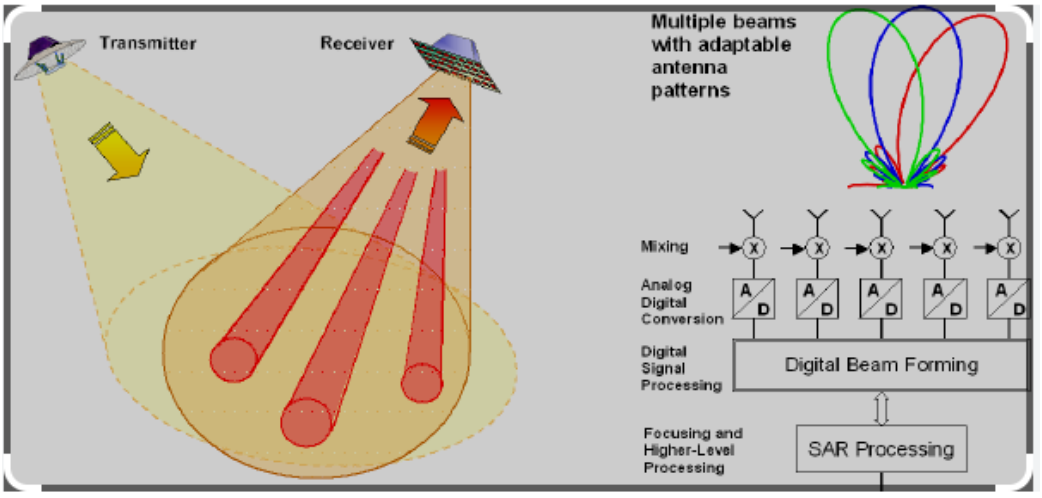

Fig 3.1. Beamforming at the receiver end of the radar [18].

To achieve this, an array of multiple antenna elements is employed. Each antenna element is connected to a separate receiver channel and can be individually controlled to introduce a phase

shift in the received signal. By properly adjusting the phase shifts across the array elements, the radar system can manipulate the directionality of the beam.

The basic principle behind beamforming is to ensure that the signals from different antenna elements arrive at the desired target location in phase, while signals from other directions arrive out of phase and cancel each other out. This constructive interference focuses the transmitted energy into a specific direction, enhancing the radar's sensitivity and resolution in that direction.

The use of beamforming techniques for antennas in millimeter radar application was shown to improve high-resolution sensing and detection[19].In addition, researchers continue to device new methods of antenna/sensor packaging and placement to meet up to stringent performance requirements

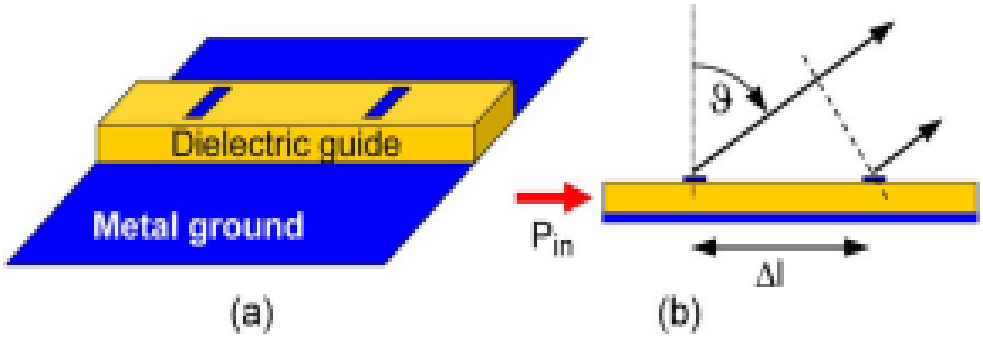

Fig 3.2. (a) Dielectric guide antenna and (b) phase angle calculation [19].

Generally, the antenna should provide not just an adequate FOV but also angle discrimination and mechanical alignment tolerances. For applications in automatic Cruise Control, it was shown that a at least 22 beams are needed for the minimum FOV while 33 will provide the necessary tolerance for mechanical alignment[20].

In order to determine the number of beams required for the antenna, the intended range, FOV and beam stack factor are needed. Overall, it was found that the specification tightness is a function of areas of application, with angle accuracy sometimes sacrificed for angle discrimination.

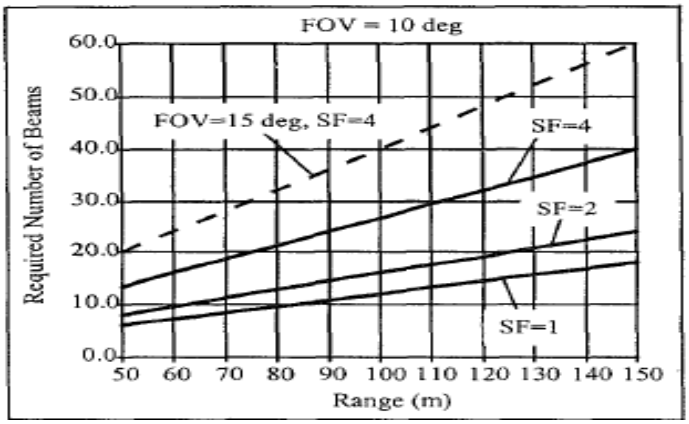

Fig 3.3. Number of Antenna Beams for ACC[20].

3.3 Radar types and estimation techniques

From the onset of radar technology, researchers realized that no single radar waveform suffices for all types of applications, for example, while long pulse radars could guarantee high range, they had shortcomings with resolving target objects that were in close proximity to each other (Range Resolution)[21]. When moving targets are the object of interest, Doppler waves are found to be ideal while slow-moving and stationary targets are best tracked by LFM waveforms.

The characterization of radar waveforms and their method of detection was reviewed [22] in the following table below:

Table 3. Radar waveforms [22].

Waveform Type	Transmit Waveform	Detection Principle	Resolution	Comment
CW	$e^{j2\pi f_c t}$	Conjugate mixing	$\Delta f_d = \frac{1}{T}$	No range information
Pulsed CW	$\prod(T_p)e^{j2\pi f_c t}$	Correlation	$\Delta R = \frac{cT_p}{2}$	Range-Doppler Performance Trade-off
FMCW	$e^{j2\pi(f_c+0.5Kt)t}$ $K = \frac{B}{T_0}$	Conjugate mixing	$\Delta R = \frac{C}{2B}$ $\Delta f_d = \frac{1}{P_{T_0}}$	Both range and Doppler information

SFCW	$e^{j2\pi f_c t} e^{j2\pi f_c t}$	Inverse Fourier transform	$\Delta R = \frac{C}{2B}$ $\Delta f_d = \frac{1}{P_{T_0}}$	Δf decides maximum range
OFDM	$\sum_{n=0}^{N-1} I(n) e^{2\pi(f_c + n\Delta t)t}$	Frequency domain channel estimation	$\Delta R = \frac{C}{N\Delta f}$ $\Delta f_d = \frac{1}{P_{T_N}}$	Suitable for vehicular communication

B denotes the Bandwidth of the radar, T is the amount of time during which data is captured

Δf is carrier /frequency separation in OFDM, N is the number of samples in CW radar and number of carriers in orthogonal frequency division multiplexing (OFDM), $\prod(T_p)$is the rectangular pulse of duration (T_p).[22].

Radars can also be categorized according to their range estimation capacity. A table containing their azimuth and elevation FOV as well as areas of application are as shown below:

Table 4 : Radar classification on the basis of their range estimation capability[22].

Radar Type	Long range Radars (LLR)	Medium Range Radars (MLR)	Short Range Radars (SRR)
Range (m)	10-250	1-100	0.15-30
Azimuthal FOV (deg)	+- 15	+- 40	+- 80
Elevation FOV (deg)	+- 5	+- 5	+- 10
Applications	Automotive cruise control	Lane-change assist, cross-traffic alert, blind-spot detection	Park assist, obstacle detection, pre-crash

There are other criteria used in radar classification, including operating frequency bandwidths. Radar systems that are used for autonomous vehicles applications are characterized by small size, low power consumption and must be robust under challenging environmental conditions. They play an important role in advanced driver-assistance systems (ADAS) , ranging from collision avoidance to stationary and moving object detection as well as imaging. The radars can be

classified according to their physical architecture, operational mode as well as their waveform types.

3.3.1 MIMO radar

Multiple input-output (MIMO) radars came about as a solution to the problem of poor angular estimation by conventional single-input-output radars. It is essentially based on the use of multiple transmitting and receiver channels simultaneously, with the effect of increasing the number of paths between the radar and the target object efficiently. In practice, the number of paths is the product of the transmitting channels and receiver channels, with the added capacity to improve the angular resolution and estimation accuracy via the arrangement of the paths into a larger virtual aperture which can then be processed using conventional array processing techniques (see figure 3.4 below):

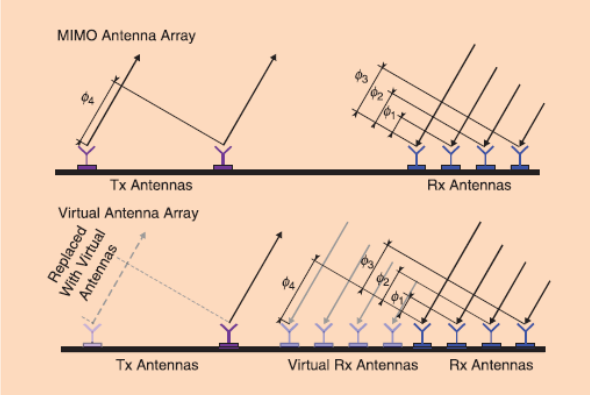

Fig 3.4. MIMO radar operation and resulting virtual apertures [23].

One of the requirements for MIMO radars is the distinguishing of signals from the different antennas and this is done by a suitable choice of signal multiplexing algorithms. One of the most popular multiplexing technique in use is the time division multiplexing (TDM)[24], with the chirps separated in equal time interval in what is known as fast –chirp radar.

Three methods exist presently for the modulation of radar transmitter signal: Time division multiplexing (TDM), frequency division multiplexing (FDM,) and code division multiplexing (CDM). The aim of any of the methods is the transmission of multiple signals which must be able to be separated at the receiver end of the radar adequately for signal processing purposes[25]. One method employed in the modulation is the use of orthogonal signals which are then transmitted

simultaneously by the receiver antenna. The FDM is the most popular modulation method[26] and thus is the one dealt with in this review. Fundamentally consisting of the transmission of identical signal separated by a frequency called shift frequency, it is characterized by chirps of very short duration whose value must be less than the maximum possible beat frequency of the down-converted signal.

3.3.2 OFDM radars

Orthogonal frequency division multiplexing (OFDM) is found in many communication schemes where strict requirements are placed on data rates and robustness to frequency-selective fading. In radar systems, OFDM results in better range resolution, target detection and the ability to cope with multipath effects[27].

OFDM radars transmit a signal whose wideband contains signals with narrowband subcarriers. The distinguishing feature of ODFM radar signal is that the subcarriers are orthogonal to each other, thus eliminating the possibility of mutual interference. This thus makes it possible for the radar to transmit and receive multiple signals simultaneously.

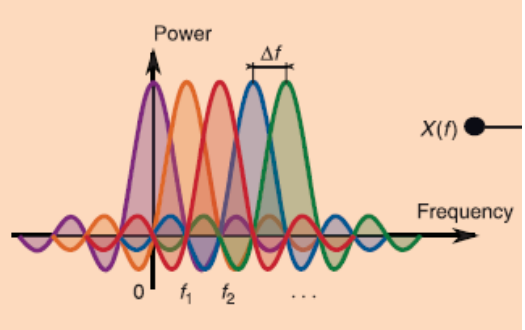

Fig 3.5. ODFM signals in the frequency domain[23].

The target objects' flight times are reflected as cyclic shifts of OFDM symbols at the receiver. After removing the cyclic prefix (CP) from the receiver signal, the OFDM symbols that have been generated through the use of IFFT are passed into the radio-frequency band(RF) using a quadrature modulation scheme and transmitted over the channel[23]. Signal processing operations lead to a sum of 2D complex exponentials, with the frequencies of the subcarriers and symbols corresponding to the distances and velocities of the radar target objects.

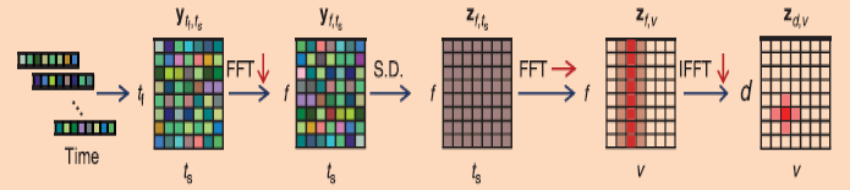

Fig 3.6. Signal processing steps of OFDM radar [10].

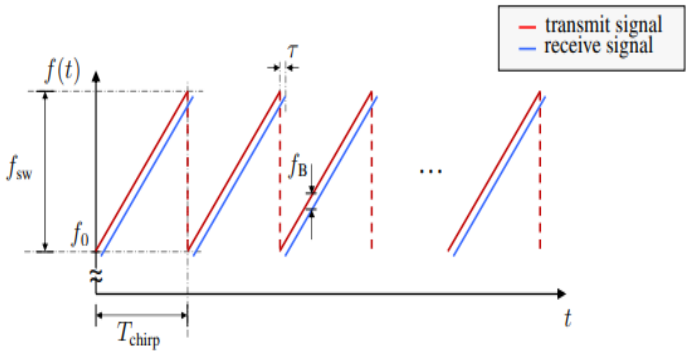

Fig 3.7. FMCW signals being transmitted and received in a sequence waveform [25].

3.3.3 Pulse radar

Pulse radar was among the earliest forms of radar waveform utilized for military applications. The technique utilized is the transmission of pulses of electromagnetic energy outwards from the antenna of the radar and then capturing and analyzing the return signal. The time delay between the pulses, the transmitted peak power and the pulse repetition frequency (PRF) are important design considerations of a pulse radar. They are relatively simpler to generate compared with other radar waveforms but have the drawbacks of relative high power supply and ‘blind spot’, a term describing the non-detection of objects during the short time that the radar transmitter and receiver are off.

3.3.4 Triangular wave radar

Triangular wave radar utilize waveforms in the form of saw-tooth waves to generate signals over a range of frequencies[28]. One advantage of this type of waveform is the possibility to operate over wider frequency ranges as well as proven robustness to interferences from clutters and signals outside of the radar antenna main lobes. The wide bandwidth feature enables the radar to perform better in resolving objects that are close together than radars that utilizes pulse waveforms.

Triangular wave radars are prone to the Doppler effect[29], a situation that directly impacts on the radar's ability to correctly estimate the range of a target object. In addition, they are prone to phase errors and are thus not utilized in applications where phase accuracy is a critical design feature.

3.4 LFM radars

LFM radars operate by transmitting a continuous-wave (CW) signal with a linearly increasing or decreasing frequency over time. The transmitted signal, known as a chirp, consists of a coherent and narrowband frequency sweep. The frequency sweep enables the radar to detect and distinguish objects at different ranges based on the received echo signals. By analyzing the time delay and Doppler shift of the returned signals, LFM radars can extract target information such as range, velocity, and angle.

The signal characteristics of LFM radars are significant for their operation. The linear frequency modulation allows for a constant rate of change of frequency with time, ensuring a predictable relationship between transmitted and received signals. This feature simplifies the signal processing required for target detection and tracking. Additionally, the bandwidth of the chirp affects the radar's range resolution, with a wider bandwidth resulting in finer resolution. LFM radars also offer good immunity to interference, as they exhibit a low range side lobe level and can suppress clutter effectively.

One of the problems that need to be addressed by modern LFM radars is that of multipath cluttering, where signals do not travel directly from target objects to the receiver, but instead take a multipath before arriving at the radar receiver[30] as shown below:

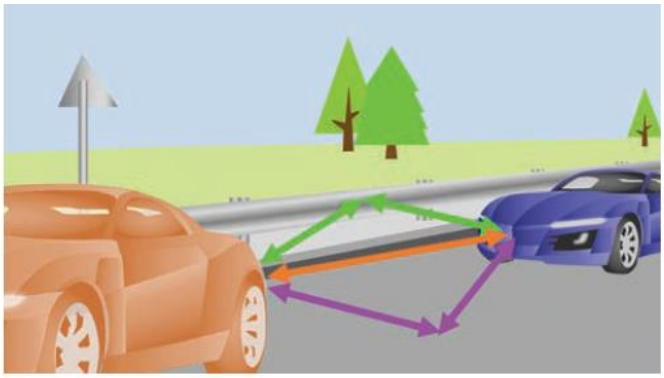

Fig 3.8. Multipath propagation can distort the range and velocity estimation of radars [30].

The challenges of automotive radars are made more challenging by the fact that all targets above the ground surface must be detected and analyzed for the proper functioning of the autonomous/semi-autonomous vehicle. In most cases however, such targets fall outside the antenna's FOV and are therefore picked up as very weak echoes[30].

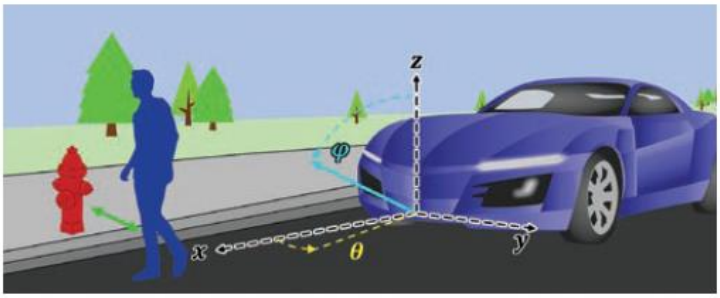

Fig 3.9. A typical clutter scenario faced by automotive LFM Radars [30].

3.4.1 Applications of LFM radars

LFM radars find extensive applications across various fields due to their favorable characteristics. One of the primary applications is in target detection and tracking. LFM radars excel in detecting and tracking moving targets, providing accurate range and velocity information. They are commonly employed in air traffic control systems, maritime surveillance, and military applications such as missile defense and airborne reconnaissance. LFM radar designers have also invented an LFM waveform that can adapt to the surroundings to mitigate multipath interferences[31]

Another prominent application of LFM radars is ground-penetrating radar (GPR). By utilizing the ability to penetrate through various materials, LFM radars can image subsurface structures and identify buried objects. GPR systems with LFM signals are used in geological surveys, archaeological studies, and infrastructure inspections.

Furthermore, LFM radars play a crucial role in weather radar systems. Their capability to measure the range and velocity of precipitation particles enables accurate weather monitoring, forecasting, and severe weather detection. LFM weather radars are instrumental in providing timely warnings for severe storms, tornadoes, and other hazardous weather events.

3.4.2 Advantages and vulnerabilities of LFM signals

LFM signals offer several advantages that contribute to their widespread adoption. Firstly, they provide excellent range resolution, enabling the detection of multiple targets at different distances.

This feature is particularly beneficial in scenarios where precise target localization is required. Secondly, LFM radars exhibit high resistance to various types of interference, including clutter and jamming signals. The predictable nature of the chirp signal simplifies the design of clutter rejection algorithms and enhances the radar's ability to extract weak target echoes.

The starting frequency of the LFM is known as the base or carrier frequency and is the lowest frequency that is transmitted. LFM signals are produced using a combination of voltage control oscillators (VCO), a phase lock loop, and a feedback system. The output is a function that increases in frequency linearly in time (chirp) whose time duration is known as sweep time in radar literature and frequency sweep known as bandwidth.

The transmitted signal, in the absence of external sources of disturbances, can be written as:

$$S_{Tx}(t) = A_{Tx} .\cos(2\pi f_0 t + \pi k t^2) \quad (10)$$
$$for\ all\ t\ \epsilon\ [0, T_{CH}]$$

In addition to being able to satisfy the long pulse width requirement for long unambiguous distance, it also simultaneously satisfies the contrasting range resolution condition due to the elasticity of the wave[32].

However, LFM radars also have vulnerabilities that should be considered. One vulnerability is the limited range ambiguity resolution due to the finite bandwidth of the transmitted chirp. In situations where multiple targets are present within the same range window, the radar may struggle to distinguish them accurately. Additionally, LFM radars are susceptible to certain types of interference, such as frequency-stepped jamming or deception techniques that exploit the linearity of the frequency sweep.

Where T_{CH} is the chirp sweep time, A_{Tx} is the amplitude of the LFM signal, f_0 is the start or fundamental frequency and k is the chirp rate.

The received signal is a diminished version of the transmitted signal with a time delay that corresponds to the distance of separation between the radar and the target object.

3.5 Interferences in LFM radars

LFM radars, frequently called CWFM radars are affected by interferences when being operated in a multi-radar environment. This interference can be caused by similar automobiles fitted with

radars operating in similar frequencies and power ranges. This situation is what is referred to as interference, with the radar of interest known as the victim radar and the radars causing the interference called interfering radars. Linear Frequency Modulation (LFM) radars are widely used in various applications, including surveillance, target tracking, and remote sensing. These radars emit signals with a linearly increasing or decreasing frequency over time. While LFM radars offer several advantages, such as high-range resolution and improved target detection, they are also susceptible to interference from external sources.

A comprehensive mathematical modeling of the equations of the interference signal, beat frequency generations as well as white noise in the receiver of the antenna was done [33].

3.5.1 Interference development

One of the figures of merit used in evaluating the performance of a radar suffering from interference is the signal to interference ratio (SIR), measured as the ratio of the transmitted power to the received interference power (see fig 3.12).

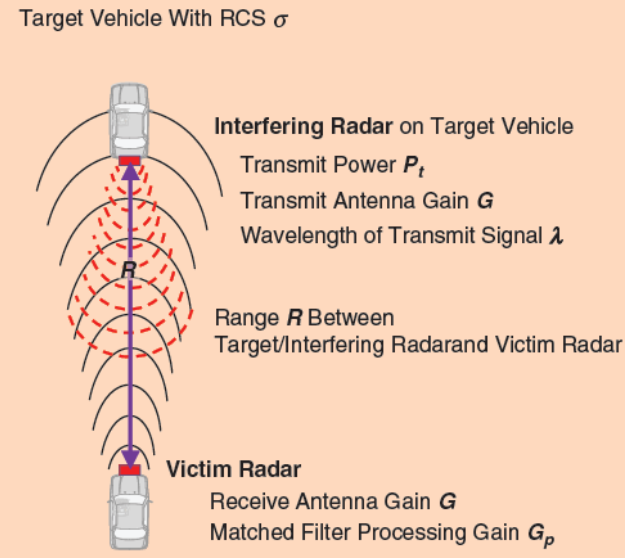

Fig 3.10. Interference scenario for automotive radar systems [33].

$$\frac{P_t}{P_I} = \frac{\sigma}{4\pi R^2} \quad \ldots\ldots\ldots\ldots\ldots\ldots\ldots\ldots\ldots\ldots (11)$$

The inclusion of a matched filter in the victim radar receiver circuit is done to improve this figure of merit, with the SIR then obtained by the expression below:

$$SIR = G_p \frac{\sigma}{4\pi R^2} \quad \ldots\ldots\ldots\ldots\ldots\ldots\ldots\ldots\ldots\ldots (12)$$

Where G_p is the gain of the matched filter in the victim radar's receiver.

One of the challenges of object detection and ranging is the wide range in the possible values of the target object's cross-sectional area(σ), which can vary from 0.001m^2 to 10m^{2,} the targets ranging from insects to buses (Table 1).To make matters worse, the RCS is not a constant parameter for a given radar target but varies according to the objects aspect ratio (The angle that the target object presents to the radar signal). This phenomenon was investigated by J.Hasch et al and they carried out experiments with radar targets using automobiles of different sizes. Their findings were that the aspect angle for different objects caused the receiver signal power to vary from between 0dBbm to 30Bsm for the same medium-sized Mazda car[34]. For FMCW and PMCW radars, the interference was found to be determined by the slope of the interference waveform.

3.5.2 Interference and target orientation and characteristics

The influence of noise contributed by clutter, electrostatic sources and other energy sources present in the communication medium must be assessed to correctly evaluate the performance of the radar system. The figure of performance known as the interference to noise ratio factors in other parameters of the interfering radar not covered by the SIR parameter. It considers the characteristics of the victim radar as well as the interfering radar as well as other signal processing methods used in the radar scheme. For an interfering radar with a bandwidth of B,the metric PSD is used to measure the interference to noise ratio of the radar and is given by the expression below

$$PSD_{INT} = \frac{[P_t G_t \lambda P_t L_{tx} l_f N_{tx}\,](D_F)\,K}{B4\lambda R^2} \quad \ldots\ldots\ldots\ldots\ldots\ldots\ldots\ldots (13)$$

It was shown that the interference to noise ratio depends on the FOV encompassing the target as well as the aspect angle presented to the transmitted wave [35] as shown below:

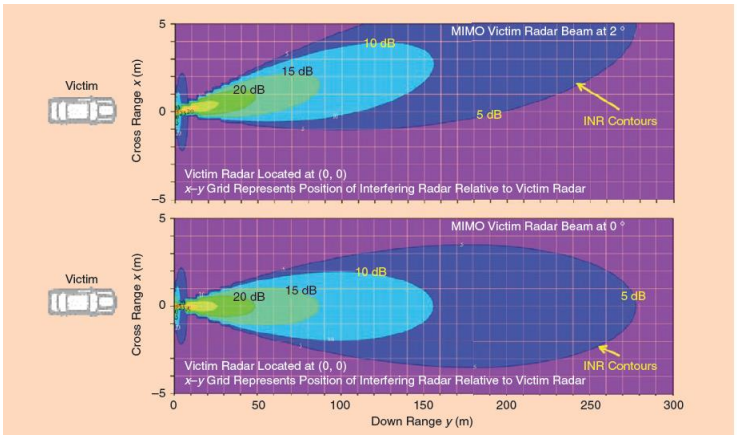

Fig 3.11: INR in a contour like map that depends on the aspect angle of target [35].

They also showed the simulation of the time-frequency domain characteristics, where the interference appeared as a spike or impulse like function in the time domain after bandpass filtering and down-conversion as shown below:

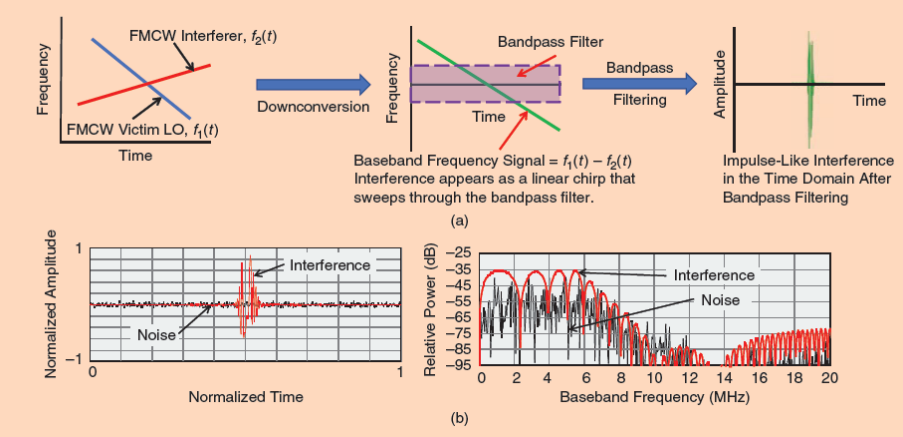

Fig 3.12 (a)Time frequency characteristics (b) Interference response in baseband [35].

The effect of the interference slope rate in the baseband of the down-converted signal was demonstrated in the paper also, with the parameter K ranging from 0.5 to the sweep bandwidth of the victim radar. It was shown that the interference usually spreads to no less than half of the bandwidth of the victim radar after down conversion.

K is defined as the ratio of the interference signal chirp BW to its BW after down conversion in the victim's radar's baseband. It depends on the FMCW sweep rate of the interference and victim radar and can be controlled by changing the slope, starting frequency and BW of the chirp

$$K = \frac{\Delta F_I^{RF}}{\Delta F_I^{BB}} \quad \ldots\ldots\ldots\ldots\ldots\ldots\ldots (14)$$

From this relationship now arises the following scenarios:

- Case 1:The start frequency, duration and start time of the victim radar is the same as the interference radar:

$$K = \left| \frac{S_I}{S_v - S_I} \right| \quad \ldots\ldots\ldots\ldots\ldots\ldots\ldots\ldots (15)$$

- Case 2: The start time, duration, and center frequency are the same.

$$K = 2 * \left| \frac{S_I}{S_v - S_I} \right| \quad \ldots\ldots\ldots\ldots\ldots\ldots (16)$$

Where S_I is the FM sweep rate of the interference radar and S_v is the FM sweep rate of the victim radar. The influence of the sweep rate is as shown below:

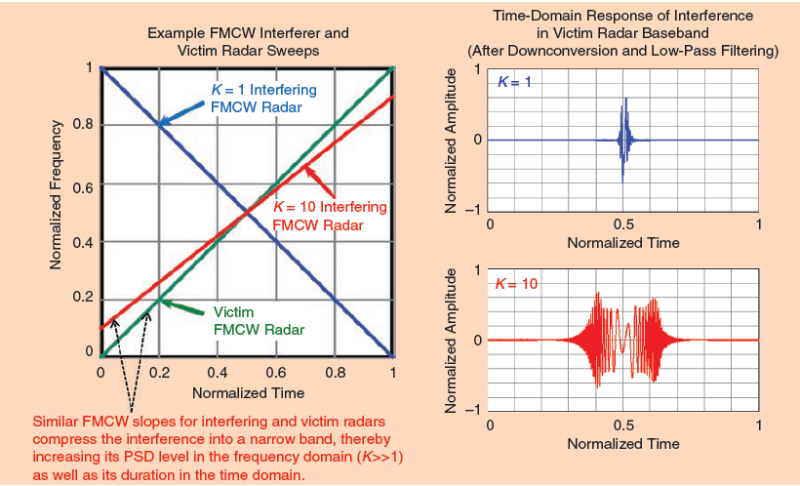

Fig 3.13. Effect of LFM slope on the PSD in the down converted signal [35].

3.6 Interference sources in LFM radars

3.6.1 Clutter Interference

Clutter refers to unwanted echoes originating from stationary or slowly moving objects within the radar's surveillance region. These echoes can mask the radar's target signals, leading to reduced detection performance. Clutter interference can arise from natural elements (e.g., trees, buildings)

or man-made objects (e.g., buildings, vehicles). Various clutter mitigation techniques have been proposed, including adaptive filtering, space-time adaptive processing (STAP), and Doppler filtering, to enhance target detection in cluttered environments.

3.6.2 Jamming interference

Jamming interference involves the deliberate transmission of strong radio frequency signals to disrupt the operation of a radar system. This interference can be generated by adversaries seeking to hide or confuse their presence. Common jamming techniques include continuous wave (CW) jamming, frequency modulated (FM) jamming, and noise jamming. To counter jamming, radar systems employ anti-jamming techniques such as frequency hopping, spread spectrum modulation, and adaptive nulling.

3.6.3 Multipath interference

Multipath interference occurs when radar signals reach the receiver via multiple paths, resulting in signal distortion. This interference can arise due to reflection, diffraction, or scattering from various objects, such as buildings, terrain features, or atmospheric conditions. Multipath interference can degrade the accuracy of target localization and tracking. Techniques such as adaptive beamforming and waveform diversity have been proposed to mitigate multipath interference and improve radar performance.

3.7 Interference mitigation techniques

A comprehensive description of interference mitigation techniques was carried out in [36].The study shows that techniques ranged from the waveform manipulation to advanced signal processing techniques[37].

3.7.1 Signal processing techniques

LFM radars employ various signal processing techniques to mitigate interference[38],[39],[40],[41][42]. These techniques include matched filtering, pulse compression, and adaptive filtering. Matched filtering enables the extraction of weak target echoes from noisy radar returns, while pulse compression enhances range resolution. Adaptive filtering techniques, such as STAP, adaptively suppress interference and clutter by exploiting the spatiotemporal statistics of the received signals.

3.7.2 Frequency and code diversity

By employing frequency and code diversity, LFM radars can reduce the effects of interference. Frequency diversity involves transmitting multiple LFM signals with different carrier frequencies, while code diversity uses different coding sequences for signal modulation. These techniques increase the resilience of the radar system against interference sources, as the probability of all signals being affected simultaneously decreases.

3.8 Simulation work on interference in a multi-radar environment

In order to check the way interference affects LFM radar performance, it was necessary to choose the signals that are most commonly deployed in automotive radar systems. These waveforms are:

- LFM signals
- Pulse LFM signals
- Triangular LFM signals
- RHLFM signals

3.8.1 Generation of different kinds of LFM-based waveforms

LFM signal sweeps a frequency range over a time interval in a linear manner. This can be in an increasing or decreasing mode while pulse LFM transmits a series of discrete pulse with each pulse increasing or decreasing in value over the transmitted period. Triangular wave is a combination of a linearly increasing LFM over a fraction of the chirp sweep time and a linearly decreasing LFM over the remainder of the sweep time. RHLFM is an LFM that uses a series of LFM chirps, each chirp beginning at a different start frequency from the predecessor but having identical sweep time over the period. LFM signals are used in determining the range and range resolution of target objects while the pulse radar is used for Doppler frequency measurements where high precision and accuracy are required. Triangular LFM are employed in surveillance systems, manufacturing where little movements and direction changes are critical. RHLFM are used for applications where security of operation is crucial, and is widely employed to counter jamming signals and interference when operating in a multi-radar environment. They are also useful in counter-stealth operations where the probability of detecting stealthy targets are improved.

A frequency/time plot of the signals are shown below:

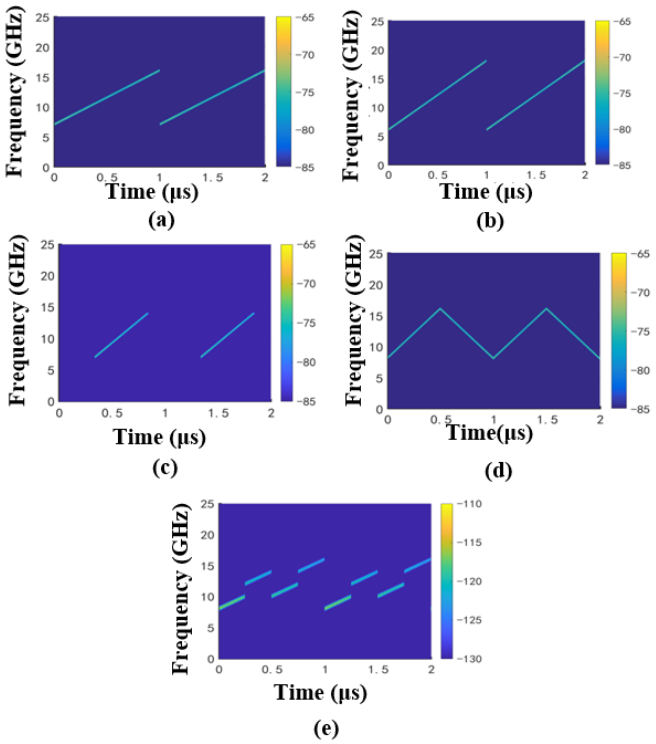

Figure 3.14. Different types of waveforms as the interference signals.

3.8.2 Objects detection without interferences

The first scenario is an interference-free situation in which the only operating radar in the vicinity is the victim's radar. In order to simulate the capabilities of this radar type to detect objects, the following scenarios have been simulated:

Two objects located at a distance of 3.5m away from the radar and 2.5m apart in an interference-free situation. The detection is made for a conventional LFM and the RHLFM as shown below:

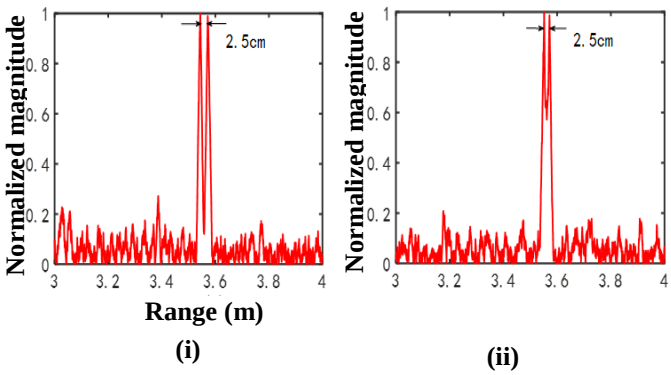

Figure 3.15. Detection of target objects by victim radars without Interference (i) LFM, (ii) RHLFM

It can be seen that both LFMs are able to detect the object at the correct position, although there is an error of a few centimeters in both detection cases.

3.8.3 Objects detection with interferences

The all familiar situation of LFM to LFM interference was first simulated. Two cars individually fitted with two distinct radar sets are envisaged. The car of interest is termed the victim radar and the car creating the interference is known as the interference radar. Two distinct cases were simulated thus:

Case 1

- LFM interference radar on LFM victim radar: In this first scenario, the slope sign and orientation of the interference and victim radar are similar. This is called coherent interference(figure 27a)
- LFM interference radar on LFM victim radar (incoherent interference): Here, the slopes of the two LFMs are opposite and dissimilar(figure 27b)
- LFM to pulse interference(fig 27c)
- LFM to Triangular wave: (fig 27d)

Case 2

- LFM interference on RHLFM victim radar (coherent)
- LFM interference on RHLFM victim radar (incoherent)
- Pulse interference on RHLFM victim radar
- Triangular wave interference on victim RHLFM signal.

The results of the simulation are shown below:

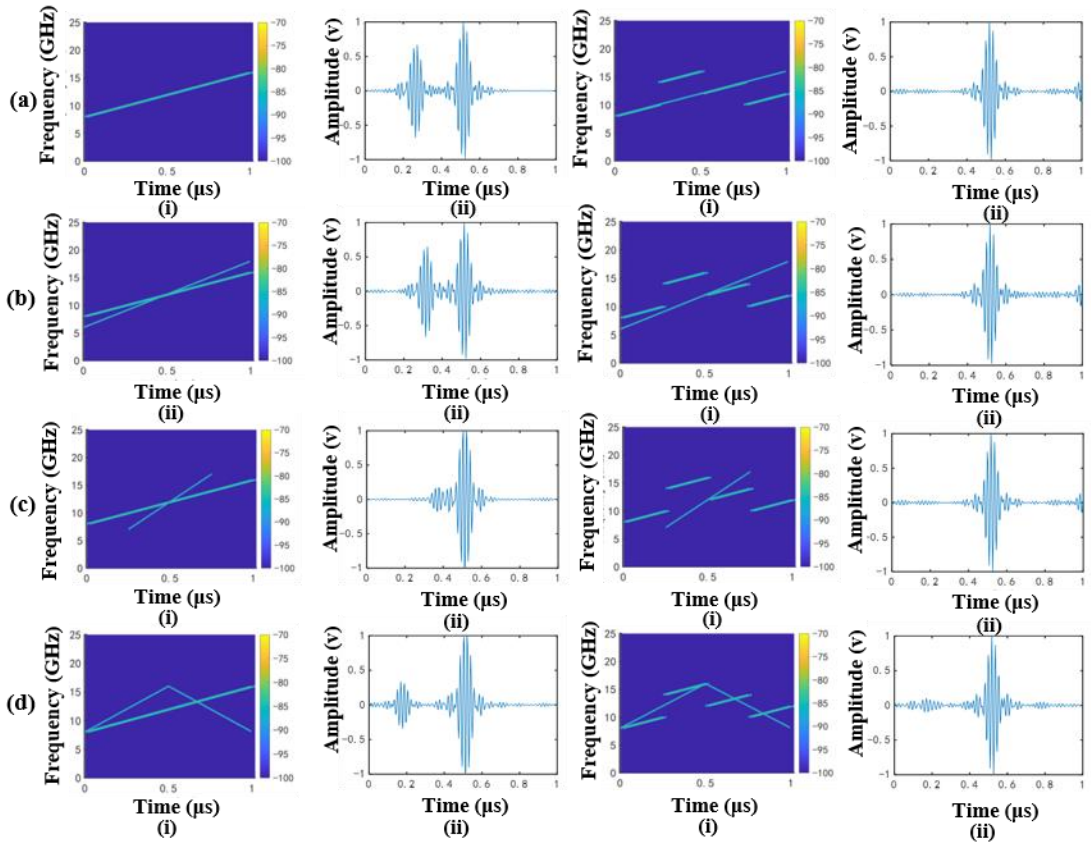

Fig 3.16. Simulation of LFM (left) and RHLFM (right), with (a) coherent interference signal, (b) non-coherent interference signal, (c) pulse interference, and (d) triangular interference waveform.

It can be seen from the figure that the interference appears as an impulse function in the receiver baseband after down-conversion and filtering. The slope of the interference signal affects the position and width of the impulse-like signal in the receiver baseband**.** When the interference signal has dissimilar, fast-crossing slopes compared to the victim signal, it covers a wide bandwidth within the victim radar's pass-band and therefore a shorter duration in the time domain**.** On the other hand, when the slope and orientation are similar (coherent), the interference is compressed into a narrow band, increasing its power spectral density in the frequency domain and extending its duration in the time domain**.** The pulse interference exhibits a shorter duration and lower intensity compared to the LFM waveform interference. In the case of triangular interference, there is a less dense impulse-like signal observed at the points where the interference signal intersects the victim radar**.** For the pulse interference, it is observed that the intensity and duration of the

impulse signal is shorter relative to the LFM case while for the saw-tooth wave, the intensity of the impulse is smallest at the point of intersection of the victim LFM and saw-tooth waveform. To mimic a real-life scenario, two objects placed 2.5cm apart are detected using the four scenarios mentioned above. The results are shown below:

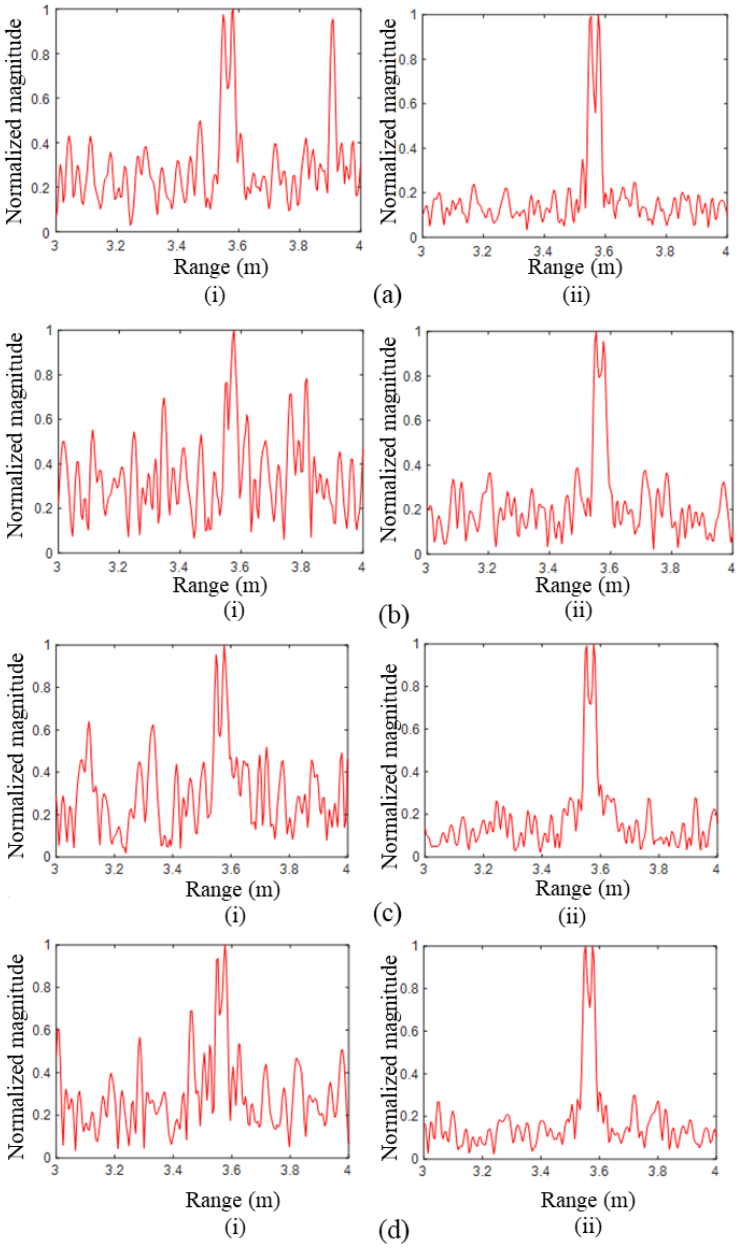

Fig 3.17. Simulated range result of target objects separated with 2.5 cm, in the presence of interference: (a) coherent interference, (b) non-coherent interference, (c) pulse-LFM interference, (d) triangle interference by victim radars: (i) LFM-based victim radar (ii) RHLFM based radar.

It can be seen that although target detection is achievable in all situations, LFM based radars have considerable challenges when it suffers from interference from similar LFMs and pulse signals. The noise floor is increased and the possibility of false detection becomes more probable. RHLFM signals however present a more robust response to all forms of interferences.

3.9 Summary of chapter

The generation of LFM has been shown to take different waveforms. Four types, namely: continuous LFM, pulse LFM, triangular LFM and RHLFM were generated and their application in many domains were elucidated. The effect of interference was shown to result in an impulse-like response in the down converter baseband frequency spectrum, with its position and intensity determined by the slope and characteristics of the interfering and victim's radar. The response of the LFM waveform was analyzed for interference/interference free scenarios for both conventional LFM and RHLFM in terms of target detection.

Chapter 4 – Millimeter Wave Radar Setup Configuration & Experiment

Texas Instrument millimeter wave radar sensors operate in the 77-81GHZ range. Already a popular choice in many automotive industry application, its configuration and deployment serves as a demonstration of the effectiveness of the radar as a sensor in critical areas of operation.

4.1 IWR1843 board

The Texas IWR1843 is a cutting-edge radar sensor system-on-chip (SoC) developed by Texas Instruments. It integrates advanced signal processing algorithms and features, making it highly suitable for various applications, including industrial automation, robotics, automotive safety systems, and smart cities. It operates in the mmWave frequency band, typically around 77-81 GHz. This frequency range allows for high-resolution sensing and imaging, with the ability to detect small objects and provide accurate range and velocity measurements.

Some of its important features are:

Multiple Antenna Array: The device incorporates a multiple-input multiple-output (MIMO) antenna array, enabling beamforming and spatial processing techniques. This allows for enhanced resolution, angular estimation, and interference rejection capabilities.

Signal Processing: The IWR1843 includes a powerful digital signal processor (DSP) and hardware accelerator, enabling real-time processing of the received radar signals. The device supports advanced signal processing algorithms for target detection, tracking, and imaging.

Configurable Parameters: The IWR1843 provides flexibility through various configuration parameters and settings. These parameters include range resolution, maximum range, frame rate, chirp configuration, modulation schemes, and antenna configuration. By adjusting these parameters, users can optimize the device for specific applications and performance requirements.

4.2 Working principle

The IWR1843 operates based on the principles of frequency-modulated continuous wave (FMCW) radar. It emits continuous waveforms with a linear frequency sweep, known as chirps, and measures the time delay and frequency shift of the returned signals. The device utilizes the phase difference and amplitude of the received signals to determine the range, velocity, and angle of detected targets.

During operation, the IWR1843 emits a series of chirps and analyzes the reflected signals. By processing the received signals using advanced algorithms, such as fast Fourier transform (FFT) and Doppler processing, the device can extract valuable information about the surrounding environment, including the presence and characteristics of objects.

Fig 4.1. The millimeter wave radar sensor board.

One such successful application of this device was in people counting (census) as covered by [43].

The millimeter wave sensor is also adept at capturing images of objects in a concealed environment and can be used in certain surveillance applications as shown in this paper where a 3D image of an object was obtained [44].

The radar sensor is programmed through the interface offered by the Texas instrument website. This interface allows the user the possibility to select some operating parameters (software platform, operating frequency and display format etc).Characteristics of radar target like RCS (receiver cross section), optimal RCS at maximum unambiguous distance and range resolution can be imputed.

Table 4.1. Key parameters of the radar sensor.

Parameter	**Description**
Frequency Range	76-81 GHz
Maximum Range	300m
Azimuth FOV	±60 degrees
Elevation FOV	±10 degrees
Range Resolution	4cm
Power Consumption	1.8W
Interface Medium	SPI (Serial Peripheral Interface)

4.3 DCA 1000EVM board

To enable effective processing of radar signals and system evaluation, the DCA 1000EVM provides a wide range of functionalities.

Fig 4.2. DCA 1000 EVM (Green) attached to the IWR 1843.

Its essential characteristics include:

Data Capture at High Speed: The DCA 1000EVM can simultaneously collect high-speed raw radar data from several receiver channels. For multi-channel radar systems, it offers versatility by supporting up to 4 receivers. Real-Time Data Visualization: It seamlessly integrates with Texas

Instruments' mmWave software development kit (SDK) and mmWave radar algorithm library, providing access to a wide range of pre-built radar signal processing algorithms in real time. This simplifies algorithm development and accelerates system evaluation.

Extensive Software Support: The DCA 1000EVM comes with software tools and libraries that facilitate data capture, configuration, visualization, and analysis. It includes a graphical user interface (GUI) for easy setup and control, as well as APIs (Application Programming Interfaces) for programmatic access and integration with custom software applications.
The board is used alongside the aforementioned IWR1843 as shown in Fig. 4.2.

The table below shows some important operating parameters of the data capture board.

Table 4.2 Summary of Data Capture Board Parameters.

Parameter	**Description**
Supported Frequency Range	76-81 GHz
Number of Receiver Channels	Up to 4 channels
Maximum Data Capture Rate	Up to 100 MSPS (mega samples per second)
Data Interface	Gigabyte Ethernet
Supported Data Format	Raw ADC Samples, Range-Doppler Maps, Range-Azimuth Heat maps
Operating Voltage	5V
Target Applications	Automotive Radar Systems, Industrial Automation, Surveillance

4.4 Experimental work

The sensor unit comes with some system defined parameter values, such as accuracy and range resolution for different operating frequencies. These parameters values fluctuate as a function of operating conditions. As much as possible, we tried to reduce the effect of random interferences

on the radar unit performance through controlled environment i.e. padding the walls and solid surfaces in the radar vicinity as well as using objects with good reflectivity for our experiment.

4.4.1 Radar sensor performance evaluation and target detection

The IWR 1843 radar alongside the DCA 1000 EVM evaluation board were configured and connected together to test the accuracy and detection of stationary objects in their operating range. In the experiment, two frequency bands (77-81 GHz and 76-77GHz) were used alternatively to measure the target object's range and range resolution. This way, radar range equation and range resolution equations were verified experimentally.

Four platforms are available for configuring the IWR1843 ie. The application must connect to the correct device. The option chosen is that to which our device is a sub-component i.e. xWR18xx_AOP. The device must then be configured to run in the system hardware setting to be added as an external device or an extension to the PC hardware.

For the plot function, functionalities like range profile, scatter plot and noise figure can be selected. For our purpose, we disabled the range Doppler map as well as range azimuth heat map since the experiment at this stage is to verify the range and range resolution equations only. The experimental setting is as shown below:

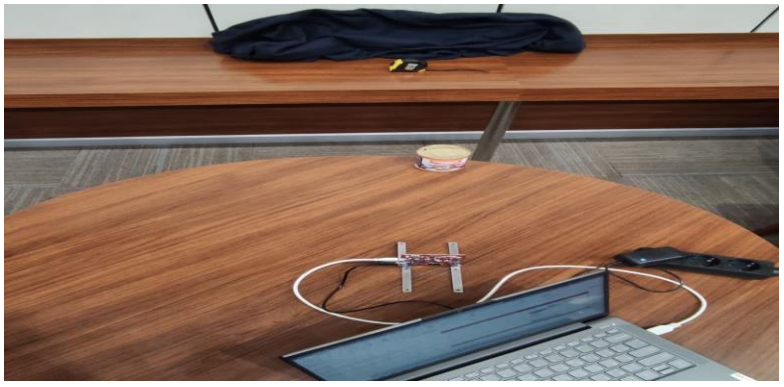

Fig 4.3. Millimeter wave radar setup to track object detection.

4.5 Evaluating the radar accuracy

Before being put to use, it is important that the radar sensor be calibrated in order to determine the limit of detection, error in reading and consistency. The table below shows the actual versus estimated distances of the radar sensor.

Table 4.3 Object detection accuracy of sensor.

BW (GHz)	Description	Radar-Object(m)	Radar to wall (m)	Range Resolution
77-81	Simulation Distance Evaluation	1.5697	2.5725	1.01
	Actual Distance	1.5	2.5	1
	Width of Spike	1.7004-1.4825	2.7033-2.3981	
	Error	0.06	0.07	0.01

Work was then carried out to ascertain the range resolution of the radar unit as shown below:

Fig 4.4. Determining the range resolution of the unit.

Using the equation $R_{res} = \frac{c}{2B}$, where c is the speed of light in vacuum and B is the operating bandwidth, we calculated the theoretical value of R_{res} as shown in the table below:

Table 6. Range resolution computation for the radar unit for three different frequency levels.

Bandwidth (GHz)	Theoretical Range Resolution (cm)	Actual Range resolution (cm)
0.9	16.00	67
1.8	8.30	35
3.6	4.17	20

The 1D range detection spectrum is as shown below for an object 4m away from the radar without interference.

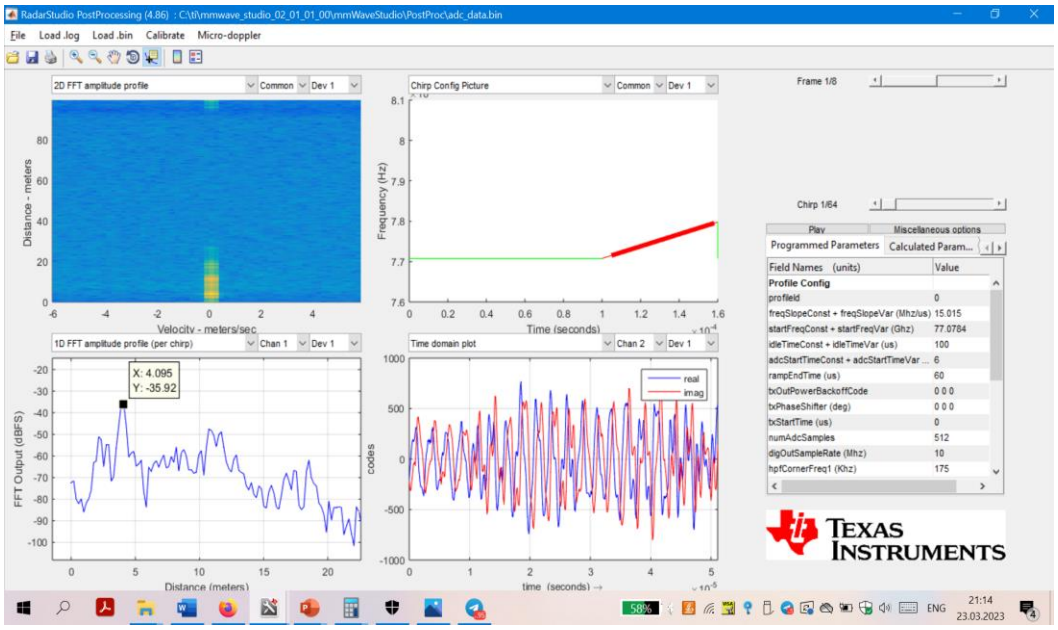

Fig. 4.5 Range profile appears as peaks in the FFT.

4.6 Summary of chapter

The IWR1843 and DCA 1000 EVM serves as the sensor and data capture board for our 1D range estimation experiments. The sensor was correctly configured and brought to operational status by closing following the manual instructions. Finally, the accuracy of measurements as well as the range resolution were ascertained experimentally.

Chapter 5- Imaging of the Detected Objects

5.1 Radar imaging

Millimeter wave (mmWave) radar systems have gained significant attention in recent years due to their ability to provide high-resolution imaging and penetration through various materials[45]. Back projection imaging techniques have emerged as a popular method for mmWave radar imaging due to their simplicity and effectiveness. This literature review aims to explore the advancements and applications of back projection imaging techniques for mmWave radar systems.

5.1.1 Back projection algorithm

Back projection imaging is a technique used to reconstruct an image from radar measurements by back propagating the received signals to their respective source locations[46]. In mmWave radar systems, back projection imaging relies on the assumption that the radar signals propagate in straight lines, enabling the estimation of the target's position and reflectivity. Incoherent Back Projection (IBP) [47]is a widely used image reconstruction technique in various fields, including medical imaging, synthetic aperture radar (SAR)[48], and computed tomography (CT). It is a relatively simple and intuitive algorithm that is computationally efficient compared to some more advanced techniques.

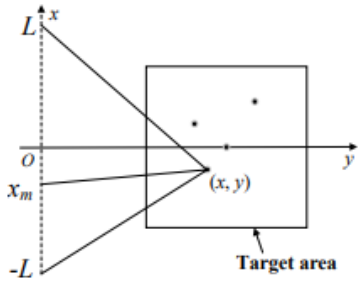

Fig 5.1. Traditional back projection method.

The basic principle of BP involves integrating the projections acquired from different angles to reconstruct an image[49]. In medical imaging, for example, X-ray projections taken from multiple angles around the patient's body are combined to create a 2D or 3D image. Similarly, in SAR,

radar measurements acquired from different positions and viewing angles are integrated to generate an image of the observed scene (see fig 5.1).

The BP algorithm works by back-projecting the acquired projections onto a reconstruction grid. Each projection is weighted and then added to the appropriate locations in the grid based on the position and orientation of the projection. The weighted back-projection process is performed for all projections, and the accumulated values in the reconstruction grid form the final image.

The object image is obtained through the superposition of pixel points on a 2D plane according to the delay time from the radar transmitter to the target object and back as in the following equations:

$$\tau = \frac{2\sqrt{(x_m - x)^2 + y^2}}{c} \qquad \ldots\ldots\ldots\ldots\ldots\ldots \qquad \ldots..(13)$$

Where c is the speed at which the wave propagates itself in air.

For a transmitted signal from the radar $p(t)$,the received signal is a delayed version of the transmitted signal alongside some attenuation and can thus be written as:

$$S(t) = \sigma . P(t - \tau) \qquad \ldots\ldots\ldots\ldots\ldots.. \qquad \ldots\ldots(14)$$

Where σ is the RCS of the target object. In order to perform a 1D –range of the target area, the conjugate of the transmitted signal is multiplied by the received signal thus:

$$r(t) = p(t) *. s(t) \qquad \ldots\ldots\ldots\ldots\ldots\ldots \qquad \ldots\ldots.(15)$$

One of the key characteristics of BP is its incoherence, meaning that it does not assume any specific coherence or phase relationships between the projections. This makes IBP more suitable for situations where the imaging system or the object being imaged exhibits incoherent or partially coherent behavior.

While IBP offers simplicity and computational efficiency, it does have limitations. One of the major challenges is the presence of artifacts in the reconstructed images. These artifacts can arise due to various factors, such as limited projection data, noise, and imperfections in the imaging system. Artifacts can manifest as streaks, blurring, or distortions, and they can degrade the image quality and affect the accuracy of the reconstruction.

5.1.2 Advancements in back projection imaging techniques

Multi-Static Configurations: Back projection imaging techniques have been extended to multi-static mmWave radar configurations, where multiple receivers are used to capture the reflected signals from different angles[50]. By combining the information from multiple receivers, it is possible to improve the accuracy and resolution of the reconstructed images, particularly in scenarios with complex target geometries.

Non-Uniform Sampling: Traditional back projection imaging techniques assume a uniform sampling grid for reconstructing the images[51]. However, in mmWave radar systems, non-uniform sampling is often employed to optimize the spatial resolution and improve imaging quality. Non-uniform sampling schemes, such as compressed sensing and adaptive sampling[50], have been integrated with back projection techniques to achieve higher resolution and reduce the number of required measurements.

Motion Compensation: In practical scenarios, both the radar platform and the target may be in motion, leading to image distortions and blurring. Motion compensation techniques have been developed to mitigate these effects by accurately estimating and compensating for the target and platform motions. By incorporating motion compensation algorithms into back projection imaging, it is possible to obtain clearer and sharper images, even in dynamic environments.

5.1.3 Applications of back projection imaging in mmWave radar

Automotive Imaging: Back projection imaging techniques are extensively used in automotive radar systems for object detection and collision avoidance. By reconstructing high-resolution images of the surrounding environment, mmWave radar systems can provide valuable information for advanced driver assistance systems (ADAS) and autonomous vehicles.

Security and Surveillance: Back projection imaging has applications in security and surveillance systems, where mmWave radar can detect and track individuals or objects in real-time. By reconstructing images of the scene, mmWave radar systems can aid in monitoring crowded areas, detecting unauthorized intrusions, and enhancing situational awareness.

Medical Imaging: Back projection imaging techniques have also been explored in mmWave radar-based medical imaging applications[49]. mmWave radar can penetrate clothing and some biological tissues, allowing for non-invasive imaging of the human body. Back projection imaging

can reconstruct images that provide insights into internal structures, aiding in the diagnosis and monitoring of medical conditions.

5.1.4 Hamming window algorithm

The hamming window is used to improve the image resolution quality by masking the edges of the shape outline and intensifying the central parts of the outline. It, therefore, acts as a mask that enhances the image quality through an appropriate increase and decrease in intensity as we progress along the outline of the image. Mathematically, it can be written as follows:

$$w_n = 0.5 - 0.46 * \cos(2\pi n/(N-1)) \quad \ldots\ldots\ldots\ldots\ldots\ldots \quad (16)$$

Where w_n is the weight assigned to each data point, n is the index of the data point ranging from 1 to N (total number of data points). The Hamming window function consists of two main components: the constant term (0.54) and the cosine term. The cosine term introduces a tapering effect by varying the weights as a function of the index (n). The purpose of this tapering is to reduce the side lobes of the Fourier Transform, which helps to mitigate spectral leakage. The resulting windowed data can then be used in various image enhancement techniques, such as spectral analysis, edge detection, noise reduction, and image reconstruction

5.2 Data from back projection algorithm

Experimental data was provided by the project (Development of AI-integrated randomly hopped LFM photonic Radar for Mitigating Interferences and Attackers in Autonomous Vehicles, OPCRP2022007) research partner, Nanjing university of Aeronautics and Astronautics, China.

The experimental data stored in csv file formats were plotted. The data consisted of time amplitude columns of measured data for both transmitted and received signals. The image had already been enhanced by the use of a filtering function that acts to enhance the frequency spectrum. The implementation of equation 15 results in the intersection of the highlighted radial pixels acumulated from previous iterations ,forming the image profile as seen below**:**

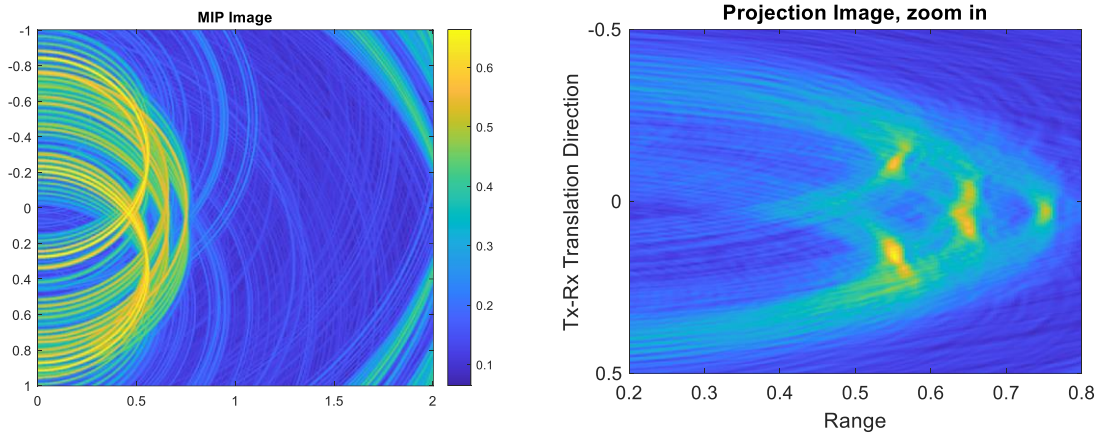

Fig 5.2: (a) Image implementation of equation 15,(b) image generation

In order to improve the algorithm, I decided to use a weighting function based on the Hamming window and obtained the following image:

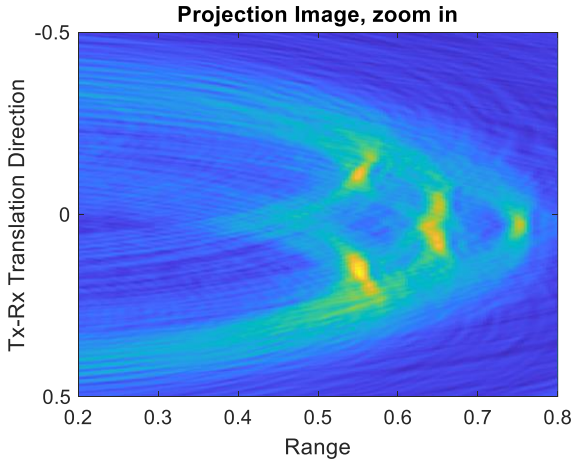

Fig 5.3. Image generation after applying hamming window

5.3 Summary of chapter

The back projection algorithm was applied to experimental data with good resolution output. Further use of the hamming window to smoothen the image had little effect because the spline smoothing function had already improved the image outline significantly.

Chapter 6 – Conclusions

The dynamics of interference produce many realities for sensors used in the automotive industry. This thesis analyzed the LFM waveform in four forms and used the generated waveform to analyze their effects when two of them interacts in a multi-radar environment.

The millimeter wave radar sensor was also used as an experimental device to directly estimate object range profile and range resolution. It was discovered that there is some 20-25cm error in range resolution accuracy contributed by non-ideal experimental conditions such as insufficient wall paddings to dampen multi-path reflections from transmitted radar signals as well as the reflectivity and geometry of experimental objects.

The image resolution was synthesized by the back projection algorithm and some improvement was sought for the final enhancement. The possibilities for enhancement was driven by the fact that the range profile which serves as the raw data for the correlation function in order to generate image pixels were not perfectly accurate. The hamming window algorithm was used due to its ability to filter out weak boundary outline and intensify spaces occupied by image object thus rendering a finer resolution. The algorithm was not able to significantly improve the final image resolution.

The future research direction is to perform experiments with the IWR1843 radar for slow velocity targets (below 10m/s) and to generate experimental data for imaging purposes and compare with those obtained through photonics generation.

References

[1] D. G. Macfarlane and D. A. Robertson, “SAFIRE: A close range real time millimetre wave radar for public education,” *IRMMW-THz2007 - Conf. Dig. Jt. 32nd Int. Conf. Infrared Millimetre Waves, 15th Int. Conf. Terahertz Electron.*, pp. 924–925, 2007, doi: 10.1109/icimw.2007.4516794.

[2] S. Hantscher *et al.*, “Security assistant system combining millimetre wave radar sensors and chemical sensors,” *IEEE Antennas Propag. Soc. AP-S Int. Symp.*, pp. 216–219, 2011, doi: 10.1109/APS.2011.5996681.

[3] G. Connan, R. Garello, H. D. Griffiths, and P. V. Brennan, “Millimeter-wave radar back-scattering from water waves,” *IEEE Natl. Radar Conf. - Proc.*, vol. 0, pp. 347–351, 2000, doi: 10.1109/radar.2000.851858.

[4] B. C. Wang, *Digital Signal Processing Techniques and Applications in Radar Image Processing*. 2008. doi: 10.1002/9780470377765.

[5] “A Study on Tunable Radio Frequency Generation Utilizing Optical Injection Locking of Single Mode Fabry Perot Laser Diodes,” 2021

[6] T. Geibig, A. Shoykhetbrod, A. Hommes, R. Herschel, and N. Pohl, “Compact 3D imaging radar based on FMCW driven frequency-scanning antennas,” *2016 IEEE Radar Conf. RadarConf 2016*, pp. 1–5, 2016, doi: 10.1109/RADAR.2016.7485168.

[7] I. Bilik, O. Longman, S. Villeval, and J. Tabrikian, “The Rise of Radar for Autonomous Vehicles,” *IEEE Signal Process. Mag.*, vol. 36, no. 5, pp. 20–31, 2019.

[8] D. W. Wang, A. L. Chen, J. Q. Yuan, and X. Y. Ma, “Sparsity-based MIMO radar imaging method,” *Proc. 2011 IEEE CIE Int. Conf. Radar, RADAR 2011*, vol. 1, pp. 967–970, 2011, doi: 10.1109/CIE-Radar.2011.6159702.

[9] B. R. Mahafza, “Matched Filter,” *Radar Syst. Anal. Des. Using MATLAB®*, pp. 221–242, 2022, doi: 10.1201/9781003051282-6.

[10] P. Adasme, I. Soto, E. S. Juan, F. Seguel, and A. D. Firoozabadi, “Maximizing Signal to Interference Noise Ratio for Massive MIMO: A Mathematical Programming Approach,” *2020 South Am. Colloq. Visible Light Commun. SACVC 2020 - Proc.*, 2020, doi: 10.1109/SACVLC50805.2020.9129889.

[11] V. Agostini and M. Knaflitz, “An algorithm for the estimation of the signal-to-noise ratio in surface myoelectric signals generated during cyclic movements,” *IEEE Trans. Biomed. Eng.*, vol. 59, no. 1, pp. 219–225, 2012, doi: 10.1109/TBME.2011.2170687.

[12] N. U. Perez, I. Arechalde, M. Castro, A. Sendin, I. Urrutia, and J. S. Gomez, “Methodology and Power Spectral Density Limits Proposal for Non Intentional Emissions in frequencies below 150 kHz,” *2020 IEEE Int. Symp. Power Line Commun. its Appl. ISPLC 2020*, pp. 0–4, 2020, doi: 10.1109/ISPLC48789.2020.9115401.

[13] R. M. Howard, “Power Spectral Density of Standard Random Processes—Part 2,” *Princ. Random Signal Anal. Low Noise Des.*, pp. 179–205, 2003, doi: 10.1002/0471439207.ch6.

[14] T. I. Popa, G. Federico, A. B. Smolders, and D. Caratelli, “Dual Rampart Antenna for Radar Systems with Enlarged Field of View,” *2022 IEEE Int. Symp. Antennas Propag. Usn. Radio Sci. Meet. AP-S/URSI 2022 - Proc.*, no. 1, pp. 185–186, 2022, doi: 10.1109/AP-S/USNC-URSI47032.2022.9887223.

[15] J. Zeng, K. Huang, and S. Ta, “A LC Resonator Based Low-pass Filter Embedded in LTCC Substrate,” *IEEE Int. Work. Electromagn. Appl. Student Innov. Compet. iWEM 2021 - Proc.*, vol. volume1, pp. 1–2, 2021, doi: 10.1109/iWEM53379.2021.9790372.

[16] B. Schoettle, “Sensor Fusion: a Comparison of Sensing Capabilities of Human Drivers and Highly Automated Vehicles,” *Sustain. Worldw. Transp.*, no. SWT-2017-12, pp. 1–42, 2017.

[17] J. Grayned, “Sae International Levels of Autonomous Driving/ Sensor Packages,” no. 3, 2019, doi: 10.4271/j3016.

[18] G. Krieger, H. Fiedler, D. Hounam, and A. Moreira, “Analysis of System Concepts for Bi- and Multi-Static SAR Missions,” *Int. Geosci. Remote Sens. Symp.*, vol. 2, no. September, pp. 770–772, 2003, doi: 10.1109/igarss.2003.1293912.

[19] W. Menzel and A. Moebius, “Antenna concepts for millimeter-wave automotive radar sensors,” *Proc. IEEE*, vol. 100, no. 7, pp. 2372–2379, 2012, doi: 10.1109/JPROC.2012.2184729.

[20] S. W. Alland, “Antenna requirements and architecture tradeoffs for an automotive forward looking radar,” *IEEE Natl. Radar Conf. - Proc.*, no. May, pp. 367–372, 1998, doi: 10.1109/nrc.1998.678029.

[21] H. E. Hassan, “Deinterleaving of Radar Pulses in a dense emitter environment,” *2003 Proc. Int. Conf. Radar, RADAR 2003*, pp. 389–393, 2003, doi: 10.1109/RADAR.2003.1278773.

[22] S. M. Patole, M. Torlak, D. Wang, and M. Ali, “Automotive Radars: A review of signal processing techniques,” *IEEE Signal Process. Mag.*, vol. 34, no. 2, pp. 22–35, 2017, doi: 10.1109/MSP.2016.2628914.

[23] “High-Performance-Automotive-Radar.pdf.”

[24] L. L. Xue and B. Ozpineci, “Adaptive time-division multiplexing driving system for solid state lighting with multiple tunable channels,” *Conf. Proc. - IEEE Appl. Power Electron. Conf. Expo. - APEC*, pp. 2830–2835, 2021, doi: 10.1109/APEC42165.2021.9487145.

[25] A. Zwanetski, M. Kronauge, and H. Rohling, “Waveform design for FMCW MIMO radar based on frequency division,” *Proc. Int. Radar Symp.*, vol. 1, no. Cdm, pp. 89–94, 2013.

[26] M. Teruya and K. Chinen, “1550nm wavelength division multiplexing and frequency division multiplexing in radio-over-fiber transmission using OFDM signals,” *Asia Commun. Photonics Conf. ACPC 2014*, pp. 1–3, 2014, doi: 10.1364/acpc.2014.ath2e.4.

[27] Y. Liu, G. Liao, and Z. Yang, “Range and angle estimation for MIMO-OFDM integrated radar and communication systems,” *2016 CIE Int. Conf. Radar, RADAR 2016*, pp. 1–4, 2017, doi: 10.1109/RADAR.2016.8059539.

[28] W. Xu, B. Wang, M. Xiang, C. Song, Z. Wang, and W. Li, “The application of Triangle Wave Signal in UAV SAR imaging,” *2021 CIE Int. Conf. Radar*, pp. 180–183, 2023, doi: 10.1109/radar53847.2021.10027895.

[29] Y. Zhang, Y. Guo, and Z. Chen, “Range-Doppler domain signal processing for medium PRF ubiquitous radar,” *2016 CIE Int. Conf. Radar, RADAR 2016*, pp. 1–4, 2017, doi: 10.1109/RADAR.2016.8059428.

[30] “The Rise of Radars for Autonomous Vehicles.pdf.”

[31] M. Picciolo, J. D. Griesbach, and K. Gerlach, “Adaptive LFM waveform diversity,” *2008 IEEE Radar Conf. RADAR 2008*, vol. i, no. 1, pp. 1–6, 2008, doi: 10.1109/RADAR.2008.4721067.

[32] P. Martelletti, *Editor-in-Chief’s 2006 report*, vol. 7, no. 1. 2006. doi: 10.1007/s10194-006-0268-4.

[33] Y. Li, B. Feng, and W. Zhang, “Mutual Interference Mitigation of Millimeter-Wave Radar Based on Variational Mode Decomposition and Signal Reconstruction,” *Remote Sens.*, vol. 15, no. 3, 2023, doi: 10.3390/rs15030557.

[34] J. Hasch, E. Topak, R. Schnabel, T. Zwick, R. Weigel, and C. Waldschmidt, “Millimeter-wave technology for automotive radar sensors in the 77 GHz frequency band,” *IEEE Trans. Microw. Theory Tech.*, vol. 60, no. 3 PART 2, pp. 845–860, 2012, doi: 10.1109/TMTT.2011.2178427.

[35] “Interference In Automotive Radar Systems - Uhnder PDF Documents Free.” [Online]. Available: https://mopdf.com/documents/25222_interference-in-automotive-radar-systems-uhnder.html

[36] S. Neemat, O. Krasnov, and A. Yarovoy, “An interference mitigation technique for FMCW radar using beat-frequencies interpolation in the STFT domain,” *IEEE Trans. Microw. Theory Tech.*, vol. 67, no. 3, pp. 1207–1220, 2019, doi: 10.1109/TMTT.2018.2881154.

[37] Z. Xu, Y. Wang, J. Luo, M. Che, H. Wang, and D. Zhang, “Potential of Reducing FMCW Radar Mutual-interference Using Nonlinear FM Signals,” *2021 CIE Int. Conf. Radar*, no. 2, pp. 2852–2855, 2023, doi: 10.1109/radar53847.2021.10028399.

[38] L. Yulan, S. Wang, and C. Shan, “High speed radar data acquisition and processing system,” *Int. Conf. Signal Process. Proceedings, ICSP*, vol. 1, pp. 449–452, 1996, doi: 10.1109/icsigp.1996.567299.

[39] W. Sun, L. Lan, G. Liao, and J. Qi, “Compound Interference Suppression for Bistatic FDA-MIMO Radar Based on Joint Two-Stage Processing,” *Proc. IEEE Sens. Array Multichannel Signal Process. Work.*, vol. 2022-June, pp. 375–379, 2022, doi: 10.1109/SAM53842.2022.9827793.

[40] B. J. Skinner, J. P. Donohoe, and F. M. Ingels, “Gradient descent method for designing optimum radar signals,” *IEEE Natl. Radar Conf. - Proc.*, pp. 67–71, 1995, doi: 10.1109/radar.1995.522521.

[41] M. Li, Y. Wu, S. J. Wu, and W. M. Yuan, “Implementation of an parallel signal processing system for all-purpose radar,” *Int. Conf. Signal Process. Proceedings, ICSP*, vol. 2, pp. 1465–1468, 2002, doi: 10.1109/ICOSP.2002.1180070.

[42] J. Xiong, G. Liao, and S. Wu, “Recursive algorithm of adaptive weight extraction of space-time signal processing for airborne radars,” *CIE Int. Conf. Radar Proc.*, pp. 86–90, 1996, doi: 10.1109/icr.1996.573778.

[43] S. Using, S. P. Handled, P. Cloud, D. C. Configuration, and G. T. Algorithms, “People Tracking and Counting Reference Design Using mmWave Radar Sensor,” no. March, pp. 1–31, 2018.

[44] M. E. Yanik, D. Wang, and M. Torlak, “3-D MIMO-SAR Imaging Using Multi-Chip Cascaded Millimeter-Wave Sensors,” no. 1, 2019.

[45] G. Sun, F. Zhang, J. Kong, X. Yu, J. Li, and S. Pan, “Photonics-based array radar imaging using an optically injected semiconductor laser,” *3rd China Int. SAR Symp. CISS 2022*, no. 2021, pp. 1–4, 2022, doi: 10.1109/CISS57580.2022.9971388.

[46] P. C. Nan, “an Implementation of the Back-Projection Algorithm According To Santosa and Vogelius,” *Symp. A Q. J. Mod. Foreign Lit.*, vol. 1, no. 2, pp. 1–6, 2006.

[47] G. Sun, F. Zhang, and S. Pan, “Improved Incoherent Back Projection Imaging based on Self-amplitude Weighting and Multiplicative Tomography Weighting,” *2019 IEEE MTT-S Int. Wirel. Symp. IWS 2019 - Proc.*, pp. 1–3, 2019, doi: 10.1109/IEEE-IWS.2019.8803854.

[48] L. Yuan, J. Ge, K. Jiang, and Y. Yong, “Research on synthetic aperture radar imaging characteristics of point targets,” *APSAR 2009 - 2009 Asia-Pacific Conf. Synth. Aperture Radar, Proc.*, pp. 282–285, 2009, doi: 10.1109/APSAR.2009.5374150.

[49] L. Pu, X. Zhang, P. Yu, and S. Wei, “A fast three-dimensional frequency-domain back projection imaging algorithm based on GPU,” *2018 IEEE Radar Conf. RadarConf 2018*, pp. 1173–1177, 2018, doi: 10.1109/RADAR.2018.8378728.

[50] Y. S. Cho, H. K. Jung, C. Cheon, and Y. S. Chung, “Adaptive Back-Projection Algorithm Based on Climb Method for Microwave Imaging,” *IEEE Trans. Magn.*, vol. 52, no. 3, pp. 1–4, 2016, doi: 10.1109/TMAG.2015.2479358.

[51] F. D. W. Enggar, A. M. Muthiah, O. D. Winarko, O. N. Samijayani, and S. Rahmatia, “Performance comparison of various windowing on FMCW radar signal processing,” *2016 Int. Symp. Electron. Smart Devices, ISESD 2016*, pp. 326–330, 2017, doi: 10.1109/ISESD.2016.7886743.